



The Geostationary Operational Environmental Satellite (GOES) Product Generation System

*S.L. Haines, R.J. Suggs, and G.J. Jedlovec
Marshall Space Flight Center, Marshall Space Flight Center, Alabama*

The NASA STI Program Office...in Profile

Since its founding, NASA has been dedicated to the advancement of aeronautics and space science. The NASA Scientific and Technical Information (STI) Program Office plays a key part in helping NASA maintain this important role.

The NASA STI Program Office is operated by Langley Research Center, the lead center for NASA's scientific and technical information. The NASA STI Program Office provides access to the NASA STI Database, the largest collection of aeronautical and space science STI in the world. The Program Office is also NASA's institutional mechanism for disseminating the results of its research and development activities. These results are published by NASA in the NASA STI Report Series, which includes the following report types:

- **TECHNICAL PUBLICATION.** Reports of completed research or a major significant phase of research that present the results of NASA programs and include extensive data or theoretical analysis. Includes compilations of significant scientific and technical data and information deemed to be of continuing reference value. NASA's counterpart of peer-reviewed formal professional papers but has less stringent limitations on manuscript length and extent of graphic presentations.
- **TECHNICAL MEMORANDUM.** Scientific and technical findings that are preliminary or of specialized interest, e.g., quick release reports, working papers, and bibliographies that contain minimal annotation. Does not contain extensive analysis.
- **CONTRACTOR REPORT.** Scientific and technical findings by NASA-sponsored contractors and grantees.

- **CONFERENCE PUBLICATION.** Collected papers from scientific and technical conferences, symposia, seminars, or other meetings sponsored or cosponsored by NASA.
- **SPECIAL PUBLICATION.** Scientific, technical, or historical information from NASA programs, projects, and mission, often concerned with subjects having substantial public interest.
- **TECHNICAL TRANSLATION.** English-language translations of foreign scientific and technical material pertinent to NASA's mission.

Specialized services that complement the STI Program Office's diverse offerings include creating custom thesauri, building customized databases, organizing and publishing research results...even providing videos.

For more information about the NASA STI Program Office, see the following:

- Access the NASA STI Program Home Page at <http://www.sti.nasa.gov>
- E-mail your question via the Internet to help@sti.nasa.gov
- Fax your question to the NASA Access Help Desk at 301-621-0134
- Telephone the NASA Access Help Desk at 301-621-0390
- Write to:
NASA Access Help Desk
NASA Center for AeroSpace Information
7121 Standard Drive
Hanover, MD 21076-1320
301-621-0390



The Geostationary Operational Environmental Satellite (GOES) Product Generation System

S.L. Haines, R.J. Suggs, and G.J. Jedlovec

Marshall Space Flight Center, Marshall Space Flight Center, Alabama

National Aeronautics and
Space Administration

Marshall Space Flight Center • MSFC, Alabama 35812

Acknowledgments

The Geostationary Operational Environmental Satellite (GOES) Product Generation System (GPGS) is the result of many years of work with the help of many people. In particular, our appreciation goes to Paul Meyer of NASA for his work on the Man-computer Interactive Data Access System (McIDAS) Abstract Data Distribution Environment (ADDE) servers that supply the GOES data and the development and upkeep of the Web servers, Kevin Laws for helping to improve the cloud mask with his Master's Thesis work, Robert Atkinson for developing the GOES calibration, and William Lapenta of NASA for supplying the MM5 forecast on a daily basis. GPGS was developed with funding from the National Oceanic and Atmospheric Administration Office of Research and Applications under the GOES Improved Measurements and Product Assessment Program and the NASA Earth Science Enterprise.

TRADEMARKS

Trade names and trademarks are used in this report for identification only. This usage does not constitute an official endorsement, either expressed or implied, by the National Aeronautics and Space Administration

Available from:

NASA Center for AeroSpace Information
7121 Standard Drive
Hanover, MD 21076-1320
301-621-0390

National Technical Information Service
5285 Port Royal Road
Springfield, VA 22161
703-487-4650

TABLE OF CONTENTS

| | |
|---|----|
| 1. INTRODUCTION | 1 |
| 2. BACKGROUND | 4 |
| 2.1 GOES Imager and Sounder | 4 |
| 2.2 Real-Time GOES Data Ingesting and Processing | 7 |
| 3. GOES PRODUCT GENERATION SYSTEM | 9 |
| 3.1 Overview | 9 |
| 3.2 Preprocessing | 10 |
| 3.3 Processing the Retrievals | 12 |
| 3.4 Postprocessing | 40 |
| 4. GOES PRODUCT GENERATION SYSTEM FUTURE IMPROVEMENTS | 42 |
| 4.1 Radiative Transfer Algorithms | 42 |
| 4.2 Cloud Retrieval Physics | 43 |
| 4.3 Use of Ancillary Data | 43 |
| 4.4 Guess Information | 43 |
| 4.5 Portability of Code | 44 |
| APPENDIX A—ASCII DATA FILE DESCRIPTION | 45 |
| REFERENCES | 49 |

LIST OF FIGURES

| | | |
|-----|---|----|
| 1. | Example of coverage provided by (a) Imager and (b) Sounder data | 2 |
| 2. | GOES timeline chart | 4 |
| 3. | Typical scan coverage for the GOES Imager: (a) GOES-East Imager extended Northern Hemisphere scan sector and (b) GOES-East Imager CONUS scan sector | 6 |
| 4. | Typical Sounder scan coverage—GOES-East Sounder CONUS scan sector | 8 |
| 5. | GHCC GOES receiving antennas | 8 |
| 6. | A diagram depicting a broad overview of real-time GPGS | 10 |
| 7. | A diagram depicting the preprocessing unit of GPGS | 11 |
| 8. | Diagram of the processing unit of GPGS | 13 |
| 9. | Diagram of the BTH cloud algorithm | 16 |
| 10. | Daytime (1845 UTC, October 25, 2003) example of the (a) visible and (b) infrared imagery, the GPGS (c) MASK and (d) CTP product, for the same time, and (e) the color key for the MASK image | 18 |
| 11. | Nighttime (0845 UTC, October 15, 2003) example of the (a) infrared imagery and the GPGS (b) MASK and (c) CTP product. See figure 10 for the MASK color key ... | 19 |
| 12. | Examples of GOES-8 (a) uncorrected and (b) visible channel degradation corrected ALB (%), (c) uncorrected and (d) corrected INS (W/m^2), and (e) uncorrected and (f) corrected CLDALB (%) at 1545 UTC, January 14, 2003 | 21 |
| 13. | GOES-8 INS retrievals compared to SURFRAD measurements for (a) the August 29, 2000, INS and (b) the March 1, 2003, INS at Goodwin Creek, MS | 24 |
| 14. | GOES-12 INS retrievals compared to SURFRAD measurements for (a) the September 15, 2003, INS and (b) the April 24, 2003, INS at Goodwin Creek, MS | 25 |
| 15. | GOES-8 TPW retrieval error statistics as a function of retrieval time for June 17–18, 1986. For this case, the time of the first-guess field is the same as the retrieval time: (a) Mean error (bias) and (b) SD. Dashed line is the error of the first-guess TPW field, and the solid line is the error of the TPW retrieval | 30 |

LIST OF FIGURES (Continued)

| | | |
|-----|--|----|
| 16. | GOES-8 TSKN retrieval error statistics as a function of retrieval time for June 17–18, 1986. For this case, the time of the first-guess field is the same as the retrieval time: (a) Mean error (bias) and (b) SD. Dashed line is the error of the first-guess TSKN, and the solid line is the error in the TSKN retrieval. Guess errors are read from the right axis | 31 |
| 17. | Intercomparison of TSKN retrievals from the GHCC algorithm and the NESDIS algorithm over the eastern half of CONUS on September 19, 2000: (a) Statistical differences between algorithm retrievals when applied to GOES-8 Imager and (b) statistics when algorithms are applied to GOES-8 Sounder | 32 |
| 18. | Intercomparison of TSKN retrievals from the GHCC algorithm and the NESDIS algorithm over the eastern half of CONUS on September 19, 2000: (a) Statistical differences between retrievals from NESDIS algorithm applied to GOES-8 Imager and Sounder and (b) statistics when the GHCC algorithm is applied to GOES-8 Imager and Sounder | 33 |
| 19. | Comparison of TSKNs measured at the ARM Southern Great Plains site by the ground-based IRT instrument with TSKNs retrieved from GOES-8 Imager and Sounder infrared channel measurements: (a) August 18, 1999, and (b) September 1, 1999. The Imager retrievals were obtained from the GHCC algorithm while the Sounder retrievals were obtained by NESDIS | 35 |
| 20. | Comparison of early morning TSKN tendencies measured at the ARM Southern Great Plains site by the ground-based IRT with TSKNs retrieved from GOES-8 Imager and Sounder infrared channel measurements: (a) From 1345 to 1245 UTC and (b) from 1445 to 1345 UTC. The Imager retrievals were obtained from the GHCC algorithm while the Sounder retrievals were obtained by NESDIS | 36 |
| 21. | TSKN 3-hr tendencies (1245–1545 UTC) September 19, 2000. Tendencies are applied to a 12-km Lambert conformal grid using GOES-8 (a) Imager retrievals (\approx 4-km resolution) with 3- by 5-pixel smoothing, (b) Sounder retrievals (\approx 10-km resolution) single-pixel per grid assignment, and (c) Sounder retrievals (\approx 10-km resolution) with 3- by 3-pixel smoothing | 37 |
| 22. | MM5 9-m surface air verification statistics using different assimilated GOES-8 retrieval TSKN products. All data is at 12-km grid resolution but obtained from different instrument pixel resolutions and number of pixels smoothed (fig. 21): (a) Bias improvement and (b) RMS improvement. Verification statistics relative to MM5 control run | 39 |
| 23. | Examples of Web page displays of the real-time GOES products | 41 |
| 24. | An example of an ASCII file generated by GPGS | 46 |

LIST OF TABLES

| | | |
|----|--|----|
| 1. | GOES Imager spectral channels and characteristics | 5 |
| 2. | GOES Sounder spectral channels and characteristics | 7 |
| 3. | Mean absolute relative differences between GOES-8 retrieved TSKN tendencies and IRT measured tendencies | 36 |
| 4. | Description of the parameters provided in the GPGS ASCII files | 47 |

LIST OF ACRONYMS AND SYMBOLS

| | |
|-----------------|---|
| ADDE | Abstract Data Distribution Environment |
| ALB | surface albedo |
| ARM | atmospheric radiation measurement |
| AWIPS | Advanced Weather Interactive Processing System |
| BSC | bispectral spatial coherence |
| BTH | bispectral threshold and height |
| CLDALB | cloud albedo |
| CO ₂ | carbon dioxide |
| CONUS | Continental United States |
| CTP | cloud top pressure |
| DI | difference image |
| EDAS | Eta Data Assimilation System |
| FOV | field of view |
| GHCC | Global Hydrology and Climate Center |
| GOES | Geostationary Operational Environmental Satellite |
| GOESRET | GOES retrieval (Fortran program) |
| GPGS | Geostationary Operational Environmental Satellite Product Generation System |
| GVAR | Geostationary Operational Environmental Satellite variable |
| HIRS | high-resolution infrared sounder |
| INS | surface insolation |
| IRT | infrared thermometer |

LIST OF ACRONYMS AND SYMBOLS (Continued)

| | |
|---------|---|
| LW | longwave |
| MASK | cloud mask |
| McIDAS | Man-computer Interactive Data Access System |
| MD | meteorological data |
| MM5 | Pennsylvania State University/National Center for Atmospheric Research mesoscale model |
| MODIS | moderate-resolution imaging spectroradiometer |
| NCAR | National Center for Atmospheric Research |
| NCEP | National Centers for Environmental Prediction |
| NESDIS | National Environmental Satellite, Data and Information Service |
| NOAA | National Oceanic and Atmospheric Administration |
| PSU | Pennsylvania State University |
| RMS | root mean square |
| RMSE | root mean square error |
| SD | standard deviation |
| SIMRAD | simulated radiances (name of the forward radiative transfer model code) |
| SURFRAD | Surface Radiation Budget Network |
| SW | shortwave |
| TPW | total precipitable water |
| TSKN | skin temperature |
| USWRP | United States Weather Research Program |
| UTC | universal time coordinated |

NOMENCLATURE

| | |
|---------------------------------|---|
| B | Planck function |
| C | coefficient |
| D | coefficient |
| dx | differential of x (x is used as an example parameter) |
| I | upwelling radiation |
| i | pixel value |
| p | pressure |
| $-ps$ | (subscript) denotes that the parameter is evaluated at the surface pressure |
| T | temperature |
| T_{bb} | channel brightness temperature |
| T_s | skin temperature |
| U | precipitable water |
| \bar{x} | overbar denotes guess value (x is used as an example parameter) |
| Δx | finite difference of x (x is used as an example parameter) |
| δx | difference between the observed value of x and the guess/calculated value of x (x is used as an example parameter) |
| ε | emissivity |
| τ | transmittance |
| $\frac{\partial x}{\partial y}$ | the partial derivative of x with respect to y (x and y are used as example parameters) |

TECHNICAL MEMORANDUM

THE GEOSTATIONARY OPERATIONAL ENVIRONMENTAL SATELLITE (GOES) PRODUCT GENERATION SYSTEM

1. INTRODUCTION

The Geostationary Operational Environmental Satellite (GOES) Product Generation System (GPGS) is a set of computer programs designed to generate meteorological data products in real-time or case-study mode using measurements from the GOES-East Imager and Sounder instruments. GPGS became operational in the fall of 1998 at the Global Hydrology and Climate Center (GHCC) in Huntsville, Alabama, and has been generating Imager products since then. GPGS has been generating Sounder products since the summer of 2000. Initially, products were only created during daylight hours (1100–2300 UTC), but 24-hr processing began in the spring of 2002. Products generated from the Imager and/or Sounder instruments are skin temperature (TSKN), total precipitable water (TPW), cloud top pressure (CTP), cloud albedo (CLDALB), surface albedo (ALB), and surface insolation (INS). Intermediate products used to create the primary products are cloud mask (MASK) and 20-day clear-sky composite images in the visible and infrared spectral regions. During the spring of 2002, significant improvements to MASK were implemented, and the CTP product was added to the operational processing. GPGS is a work in progress, and improvements to the algorithms, the system setup, and overall format are often being made. Major changes, such as the addition of new products, are also made.

GPGS relies on several channels of data from the Imager or the Sounder. GOES data are required from the visible channel, at least two longwave infrared window channels, and one shortwave infrared window channel. GOES-12 replaced GOES-8 as the current GOES-East satellite in the spring of 2003 and only the Sounder is able to provide all of the necessary channel data for all of the products. The Imager instrument on GOES-12 does not have the second longwave channel necessary for TSKN and TPW retrievals. Therefore, depending on the current operational GOES-East satellite, the following description of products and their development may apply to the Imager and the Sounder or to just one of the instruments.

TSKN, TPW, and CTP products are generated hourly using the 45-min-past-the-hour image. The products dependent on sunlight—INS, ALB, and CLDALB—are generated from 1145 through 2345 universal time coordinated (UTC). The 45-min-past-the-hour images provide coverage over most of the Continental United States (CONUS), although the coverage of the TSKN, TPW, and CTP products is also limited by the location of model data used as a first-guess in the retrieval process. Figure 1 provides an example of the coverage of the CTP product for Imager and Sounder data. Images of all the products, plus any experimental products currently being studied, are provided at <http://www.ghcc.msfc.nasa.gov/goesprod/> and are available <2 hr after the beginning scan time of the image. The previous 15 days' images are retained on the Web page. Also on the Web page are animated, interactive movie loops for each day and each product, allowing study of the variation of these products with respect to time.

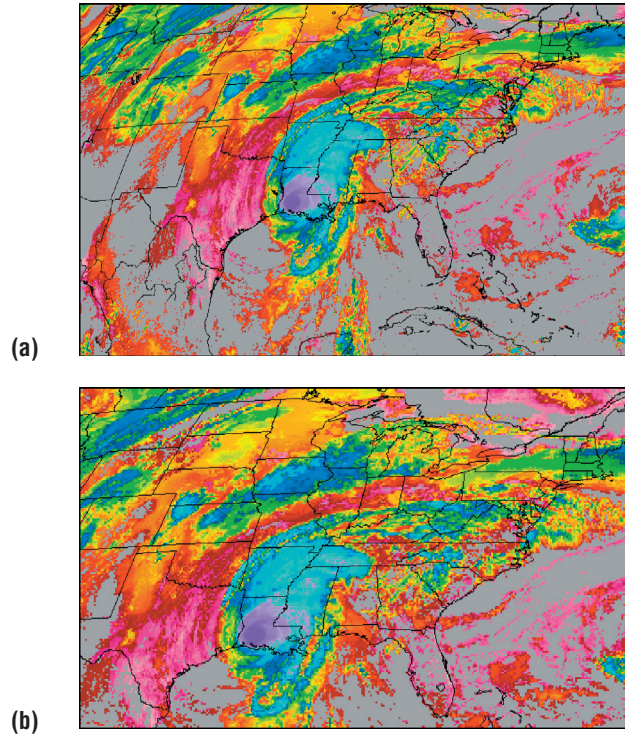


Figure 1. Example of coverage provided by (a) Imager and (b) Sounder data.

The output from GPGS is used both in house with real-time applications and for case-study work. The frequency of the retrievals allows the time rate of change (the tendency) of the TSKN product to be assimilated into numerical forecast models.^{1,2} The initial purpose of the system was to produce GOES-8 Imager products in near real time to support in-house research projects funded by the United States Weather Research Program (USWRP). The USWRP effort involved the assimilation of GOES-retrieved land surface temperature, ALB, and INS in order to improve short-term mesoscale model forecasts of surface air temperature, humidity, and precipitation. The initial phase of the project was to develop a computational system that would provide hourly GOES-retrieved products during the daylight hours in an approximate operational setup. The initial system was an integration of the then current in-house algorithms into an operational environment. The success of GPGS was a culmination of previous research and work by the Infrared Measurements Research Group at GHCC as a whole. Major milestones that were accomplished and contributed to the establishment of GPGS include the following:

- Acquisition of a GOES ground station.
- Decoding the GOES variable (GVAR) data stream and the production of Man-computer Interactive Data Access System (McIDAS) areas.
- Establishing the GHCC data server.
- MASK algorithm development work.

In addition to model assimilation, GPGS products are an important asset for meteorological applications, such as nowcasting and diagnostic studies, with several of the products being sent to the Huntsville Weather Service Office for use in their operational forecasts.³ Case-study work includes using the TSKN, INS, ALB, CLDALB, and CTP products to improve the performance of air quality models, such as the Texas 2000 Air Quality Study.⁴ The TSKN product has also been used to study the urban heat island effect.⁵

2. BACKGROUND

2.1 GOES Imager and Sounder

GOES satellites provide the near-continuous monitoring of Earth and its atmosphere necessary for intensive data analysis. They circle Earth in a geosynchronous orbit, which means they orbit the equatorial plane of Earth at a speed matching Earth's rotation, thus allowing them to remain over the same position on the surface. The geosynchronous orbit is $\approx 35,800$ km (22,300 mi) above Earth, high enough to allow the satellites a full hemispheric view. The current National Oceanic and Atmospheric Administration (NOAA) operational geostationary satellites are GOES-12 (East) and GOES-10 (West). GOES-12 is positioned at 75° W, and GOES-10 is located at 135° W. During the normal operational mode, both satellites provide views of North America up to 4 times/hr and full disk images every 3 hr.

GOES-10 and GOES-12 are the third and last, respectively, in the GOES-I through -M series.⁶ The next series of satellites GOES-N, -O, and -P will be very similar to and continue the functions of the I-M series. GOES-8 was launched in April of 1994 and served as the East satellite from shortly after its launch until it was taken out of service in April 2003. GOES-9 was launched in 1995 and initially became the new GOES-West, but failed in <2 yr and was quickly replaced by GOES-10 in July 1998. GOES-11 was launched in 2000 and remains an in-orbit spare. GOES-12 was launched in July 2001 and became the new GOES-East in April of 2003. The chronology of these satellites is presented in figure 2.

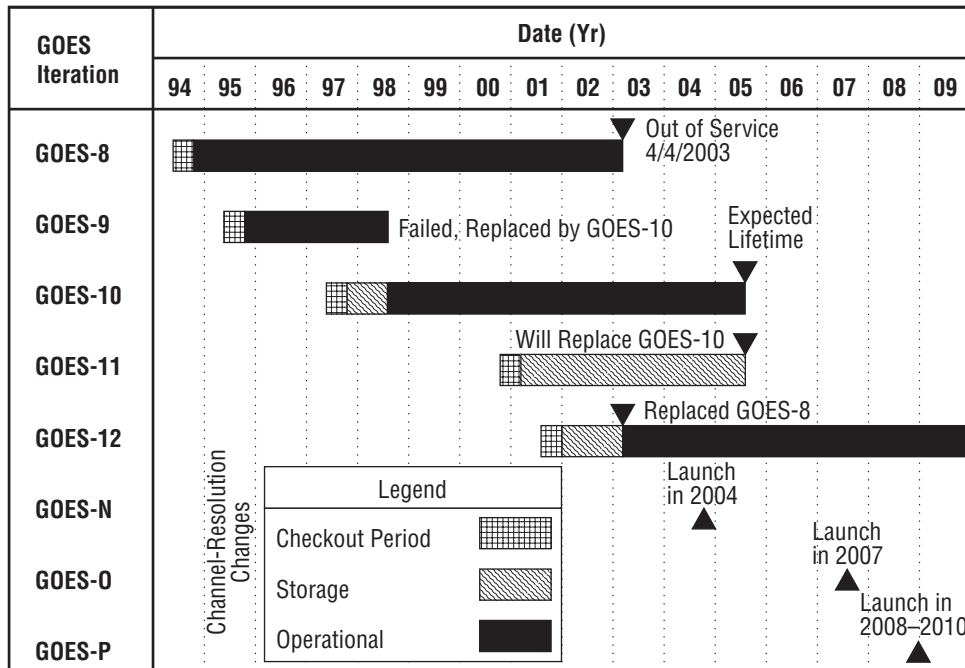


Figure 2. GOES timeline chart.

Geostationary satellites provide an important monitoring role by observing rapidly changing weather features over the hemisphere that they observe. GOES-East provides near-continuous coverage of the eastern two-thirds of North America, all of South America, and much of the tropical Atlantic Ocean, where it is a prime tool for detecting and monitoring developing tropical storms. It also serves to monitor rapidly changing cloud, atmospheric, and surface features, which are important for detecting severe storm development in the Southeast and Midwest United States. GOES-West provides coverage over much of the central and eastern Pacific Ocean and the west coast of the United States, and it is key to monitoring winter storms that form in the Gulf of Alaska and move to the west coast.

The GOES-I through -M and -N through -P series have two separate instruments for imaging and sounding. The GOES Imager is a five-channel (one visible and four infrared) imaging radiometer designed to sense radiant and solar reflected energy from sampled areas of Earth (table 1). By means of a servo-driven, two-axis gimballed mirror scanning system in conjunction with a Cassegrain telescope, the Imager’s multispectral channels can simultaneously sweep an 8-km north-to-south swath along an east-to-west-west-to-east path. Repeated scans form an image that can cover a small region at high temporal frequency or a region as large as the full disk in ≈26 min. Typical Imager coverage of the United States is presented in figure 3. The visible channel on the Imager has 1-km resolution while the short-wave and thermal infrared window channels have 4-km resolution. The midtropospheric water vapor channel has a resolution of 8 km. Beginning with GOES-12, the 12-μm window channel was replaced with a 13.3-μm atmospheric channel with 8-km resolution, and the water vapor channel resolution was increased to 4 km. The resolution of the 13.3-μm channel will increase to 4 km on GOES-O and -P.

Table 1. GOES Imager spectral channels and characteristics.

| Property | Channel No. | | | | | |
|--------------------------------------|--|--------------------|---|------------------|---|--|
| | 1 | 2 | 3 | 4 | 5 | 6 |
| | Visible | Shortwave Infrared | Water Vapor | Thermal Infrared | GOES-8, -9, -10, and -11 Thermal Infrared | GOES-12, -N, -O, and -P Thermal Infrared |
| Wavelength (μm) | 0.55–0.75 | 3.8–4 | 6.5–7 | 10.2–11.2 | 11.5–12.5 | 13.1–13.5 |
| Resolution (km) | 1 | 4 | 8 (8, 9, 10, and 11) 4 (12, N, O, and P) | 4 | 4 | 8 (12 and N) 4 (O and P) |
| Infrared Calibration | Space and internal 290 K blackbody | | | | | |
| System Absolute Calibration | Infrared <1 K Visible 5% of max scene radiance | | | | | |
| Infrared Relative Calibration | Line-to-line <0.1 K Between calibration scans 0.35 K Detector-to-detector <0.2 K Channel-to-channel <0.2 K | | | | | |
| Navigation and Registration Accuracy | Navigation accuracy 4–6 km at nadir 1-km channel-to-channel registration Within image registration 3–10 km over a 24-hr period | | | | | |

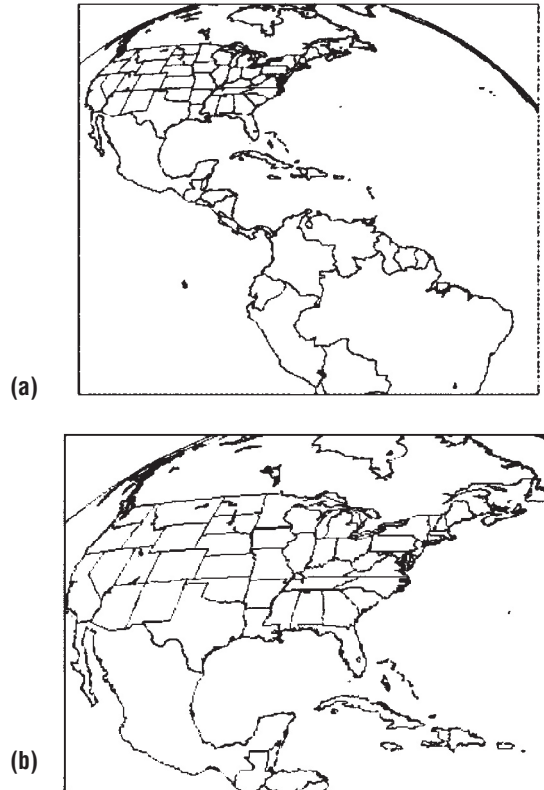


Figure 3. Typical scan coverage for the GOES Imager: (a) GOES-East Imager extended Northern Hemisphere scan sector and (b) GOES-East Imager CONUS scan sector.

The GOES Sounder is a 19-channel radiometer designed to measure upwelling radiation from Earth's atmosphere and surface in specifically designated spectral regions. These channels can be used to infer atmospheric temperature and moisture profiles as well as surface and cloud information. The spectral channels are listed in table 2. The resolution of the Sounder is 8 km at nadir, but the data are digitized at 10-km effective resolution. To improve the radiometric accuracy of data for quantitative analysis, the sensor scans much slower than the Imager, and thus, scan coverage and repetition frequencies are more limited. Figure 4 presents typical scan coverage for the GOES Sounder. The GOES Sounder remains the same throughout the GOES-I through -M and -N through -P series. Significant changes to both the Imager and the Sounder, including increases in spatial and temporal resolutions and additional channels, will be on the next generation of GOES beginning with GOES-R, currently scheduled for launch in 2012.

GPGS uses several GOES channels from the Imager or Sounder to produce TSKN, TPW, cloud, INS, and ALB products. Of particular interest are the high spatial resolution visible and infrared window channels. The visible channels of the Imager and Sounder measure the reflected solar energy from Earth's atmosphere and surface and, subsequently, are used to determine ALB, CLDALB, and INS for each GOES pixel. The GOES shortwave and longwave infrared channels are used to detect the presence of clouds and assign an estimate of their CTP at each pixel. The varying water-vapor sensitivity of the longwave infrared window channels allows for the determination of TPW and surface temperature with a physical retrieval technique. The replacement of the Imager 12- μm channel on GOES-12 with a 13.3- μm channel precludes this determination with the Imager.

Table 2. GOES Sounder spectral channels and characteristics.

| Channel | Central Wavelength (μm) | Noise (K) | Objective/Sensitivity |
|--------------------------------------|--------------------------------------|--------------------------------------|--|
| 1 | 14.71 | – | Sounding |
| 2 | 14.37 | – | Sounding |
| 3 | 14.06 | – | Sounding |
| 4 | 13.64 | – | Sounding |
| 5 | 13.37 | – | Sounding |
| 6 | 12.66 | – | Water vapor sensitivity/sounding |
| 7 | 12.02 | – | Water vapor sensitivity/surface temperature |
| 8 | 11.03 | – | Surface temperature |
| 9 | 9.71 | – | Total ozone/sounding |
| 10 | 7.43 | – | Water vapor sensitivity/sounding |
| 11 | 7.02 | – | Water vapor sensitivity/sounding |
| 12 | 6.51 | – | Water vapor sensitivity/sounding |
| 13 | 4.57 | – | Sounding |
| 14 | 4.52 | – | Sounding |
| 15 | 4.45 | – | Sounding |
| 16 | 4.13 | – | Sounding |
| 17 | 3.98 | – | Surface temperature |
| 18 | 3.74 | – | Surface temperature/sounding |
| 19 | 0.70 | – | Surface/cloud reflectance |
| System absolute calibration | – | Infrared <1 K | Visible 5% of maximum scene radiance |
| Infrared relative accuracy | Line-to-line <0.25 K | Between calibration scans 0.6 K | Detector-to-detector <0.40 K Channel-to-channel <0.29 K |
| Navigation and registration accuracy | 10-km navigation accuracy at nadir | 1-km channel-to-channel registration | Within image registration 1–5 km over a 24-hr period |

2.2 Real-Time GOES Data Ingesting and Processing

GHCC operates and maintains two satellite ground stations to receive data from the GOES Imager and Sounder instruments of the GOES-East (currently GOES-12) and GOES-West (GOES-10) satellites (fig. 5). Each ground station consists of a 12-ft mesh antenna, feed horn, power supply, and an integrated feed down converter housed in a high-end personal computer running Microsoft® Windows NT. The current systems were designed by GTI Electronics, and they run DirectMet® software for processing and displaying the GOES imagery. The ground stations receive data from the satellite and store it in GVAR data format. The data are exported to a Unix platform running McIDAS for further processing and analysis.⁷ Computer software modules developed for McIDAS at GHCC are used to convert the GVAR Imager and Sounder data streams into McIDAS area format files where standard McIDAS routines can be used to navigate, calibrate, and remap the image data. The McIDAS areas are then sent to a McIDAS server where they remain in an 18- to 24-hr revolving archive. The McIDAS

server data structure makes the GOES Imager and Sounder data available to a variety of users for further processing, including Web display, generation of near real-time data products in support of short-term forecasting, regional climate studies, and long-term storage.



Figure 4. Typical Sounder scan coverage—GOES-East Sounder CONUS scan sector.



Figure 5. GHCC GOES receiving antennas.

3. GOES PRODUCT GENERATION SYSTEM

3.1 Overview

GPGS is a set of computer programs utilizing McIDAS software and Fortran programming language connected by a series of C shell scripts within a Unix operating system. Figure 6 presents a broad overview of the real-time GPGS, with each of the ovals representing a major script, known as a driver script, and rectangles representing the major inputs and outputs of the system. The process shown in figure 6 occurs concurrently for Imager and Sounder data.

The real-time GPGS is divided into three main sections: (1) Preprocessing, which consists of the generation of the first-guess data; (2) processing, which generates the products in McIDAS area and ASCII file formats at pixel resolution and on specified grids at specified resolutions; and (3) postprocessing, which is responsible for the creation of the images for the Web page. In addition to the three main units of GPGS, there is an archiving script that moves the output from GPGS to a permanent archive.

In order for GPGS to successfully generate products, there are several required inputs. First, the preprocessing driver script needs model output profiles of temperature, pressure, and relative humidity that are valid at the operational processing time. For the real-time processing, the model output is provided by GHCC's Pennsylvania State University (PSU)/National Center for Atmospheric Research (NCAR) model (MM5) forecast. Two separate model runs provide the necessary profiles for 24 hr of product generation. The preprocessing script generates McIDAS meteorological data (MD) files of first-guess data from the model output. The processing driver script runs hourly, and requires the first-guess data provided by the preprocessing script and Imager or Sounder image data in McIDAS area format. The output from the processing unit includes McIDAS areas of the retrievals at pixel resolution and also ASCII files containing the output parameters on particular grids, including the MM5 grid configuration. These ASCII files on the MM5 grid are made available to the MM5 preprocessing for model assimilation. Once an hour, the postprocessing script uses the McIDAS areas of the products to create gif images for the Web page. The McIDAS areas, gif images, and ASCII files are all archived on a permanent storage system. Once a day the archive script moves a complete day's files to the storage system.

In case-study mode, the procedures are similar, but changes are made depending on the requirements of the particular case. First-guess data are required to make retrievals of TSKN, TPW, and CTP and may be provided from a forecast model other than the GHCC MM5 and have to be reformatted. If GHCC MM5 forecast data are to be used, normally the first-guess MD files are retrieved from the archive or the model output is regenerated. Additional preprocessing in the case-study mode includes obtaining all the necessary satellite data in McIDAS area format from the local GHCC archive or the National Climatic Data Center archive.

The processing in the case-study mode may differ from the real-time mode depending on the requirements of the case. Additional or different grids and new parameters may be required, and pixel resolution retrievals and select parameters may not be wanted. The format of the ASCII files generated in the postprocessing may differ from the format of the files generated in real time because of the differ-

ence in parameters. Also, the gif images generated may change depending on the needs of the case study. For the Texas 2000 Air Quality Study, GPGS was used to generate retrievals on several grids for a 10-day period.⁴ While pixel retrievals were not required for the study, some measure of atmospheric transmittance was required, and therefore, CLDALB was added to the GPGS suite of products. Overall, the programs used in real-time and in case-study mode are the same, and many of the same procedures are used in both modes.

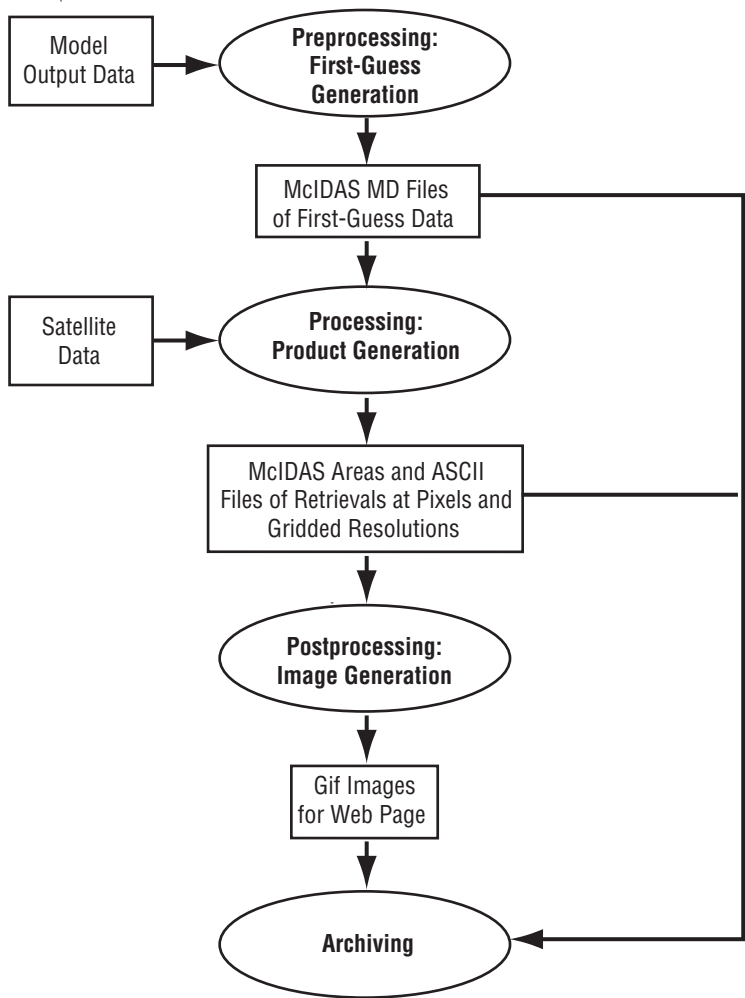


Figure 6. A diagram depicting a broad overview of real-time GPGS.

3.2 Preprocessing

The preprocessing unit is responsible for generating first-guess pressure, temperature, moisture, and perturbed transmittance profiles necessary for the TSKN, TPW, and CTP retrieval processes. The preprocessing script runs twice a day, once using the 0000 UTC GHCC MM5 forecast cycle run and once using the 1200 UTC run. The 0000 UTC run provides hourly forecasts for 1200–2300 UTC, and the 1200 UTC run provides the 0000–1100 UTC forecasts. The MM5 forecast provides hourly profiles

covering much of CONUS on the MM5 grid configuration at 36-km spatial resolution. The preprocessing script takes 4–5 hr to complete the 12-hr first-guess data; therefore, to ensure that the first-guess data are available when the processing script runs, the preprocessing script is scheduled to begin several hours before the first forecast is required. Figure 7 shows a diagram of the preprocessing unit. The driver script runs twice a day, but the Fortran program and the radiative transfer model, indicated by the ovals in figure 7, run 12 times (once for each hour) each time the driver script runs.

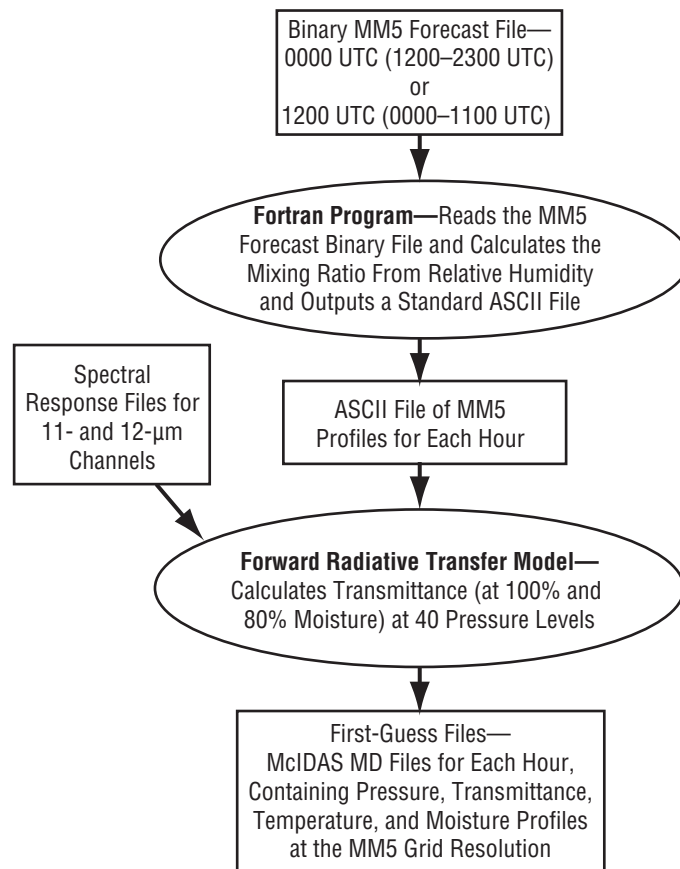


Figure 7. A diagram depicting the preprocessing unit of GPGS.

The Fortran program within the preprocessing unit requires, as input, the MM5 version 3 standard output binary file containing profiles of pressure, temperature, and relative humidity. The program outputs a reformatted ASCII file for each hour, converting relative humidity to mixing ratio in the process. The forward radiative transfer model requires, as input, the reformatted ASCII file and files containing the spectral response information of the longwave infrared window channels to be used in the TSKN and TPW retrieval process. Additional information required by the model includes the first and last wave number of the spectral region covered by the two or more spectral response files, the name of the output MD file, and the latitude and longitude of the viewing satellite. The model calculates transmittance values at 40 different pressure layers throughout the atmosphere twice: (1) Using the moisture values provided by the model data and (2) using moisture values set to 80 percent of the original values.

The two profiles are used to determine a perturbation of transmittance due to moisture change. The current model in use, SIMRAD, truncates all input profiles with pressure levels greater than 1,000 mb to 1,000 mb.⁸ The model outputs, once for each hour, a McIDAS formatted MD file containing the two transmittance profiles together with the temperature, pressure, and moisture profiles at the resolution of the MM5 configuration consistent with the view angle of the satellite instrument. This MD output file is referred to as the first-guess file.

3.3 Processing the Retrievals

The processing unit is responsible for producing 24-hr retrievals of TSKN, CTP, and TPW. The processing unit is also responsible for producing daytime (1145–2345 UTC) retrievals of ALB, CLDALB, and INS from the Imager and/or Sounder instruments on board GOES-East. The real-time processing unit runs once an hour, 24-hr/day, using the 45-min-past-the-hour satellite images available from the GHCC GOES ground station. The processing unit consists of several modules (scripts) that are all called by the driver script. Figure 8 provides a diagram of the processing driver script with each oval representing a script or module and the rectangles representing the inputs and outputs.

3.3.1 Image Update Module

The image update module begins the processing section of GPGS. The image update module acquires the necessary satellite data in McIDAS area format, updates the local 20-day archives, and creates several composite images that are required by the different modules of GPGS. The satellite data are obtained from the local GHCC GOES-East Abstract Data Distribution Environment (ADDE) server for real-time processing, or from the GHCC long-term archive of McIDAS areas in case-study mode. In each case, the data are subsetted, or cropped, from the original GOES domain to a size covering most of CONUS, with the size determined by the number of pixels and coverage determined by center location. The cropping of each area into a defined domain ensures that the areas for each channel and each time are the same in terms of coverage. Maintaining consistency in domain coverage is essential for GPGS since areas of different channels and different times are compared against each other pixel by pixel.

The required satellite data for GPGS are the visible (Imager 0.65 μm and Sounder 0.69 μm), shortwave infrared (Imager 3.9 μm and Sounder 3.7 μm), and the two longwave split-window channels (Imager 10.6 and 12 μm and Sounder 11.03 and 12.02 μm). On GOES-12, a 13.3- μm channel replaced the 12- μm split-window channel, therefore, with the transition to GOES-12 from GOES-8 in the spring of 2003, the Sounder became the only source for the two split-window channels necessary for the TSKN and TPW retrievals. However, the remaining products do not require the 12- μm channel and can therefore be produced from both Imager and Sounder data. In addition to the channel images, there are several products generated directly from the image data in this module. Four 20-day composite images representing clear-sky values of the particular image or product are generated. There are separate composite images containing the following information for each pixel at each hour:

- The minimum visible channel ALB value.
- The 11- μm longwave maximum brightness temperature.
- Two images containing the smallest positive and the smallest negative differences between the 11- and 3.9- μm channels for the 20 days.

Obviously the visible channel and the minimum ALB composite image are only obtained or generated during the daylight hours; i.e., 1145–2345 UTC.

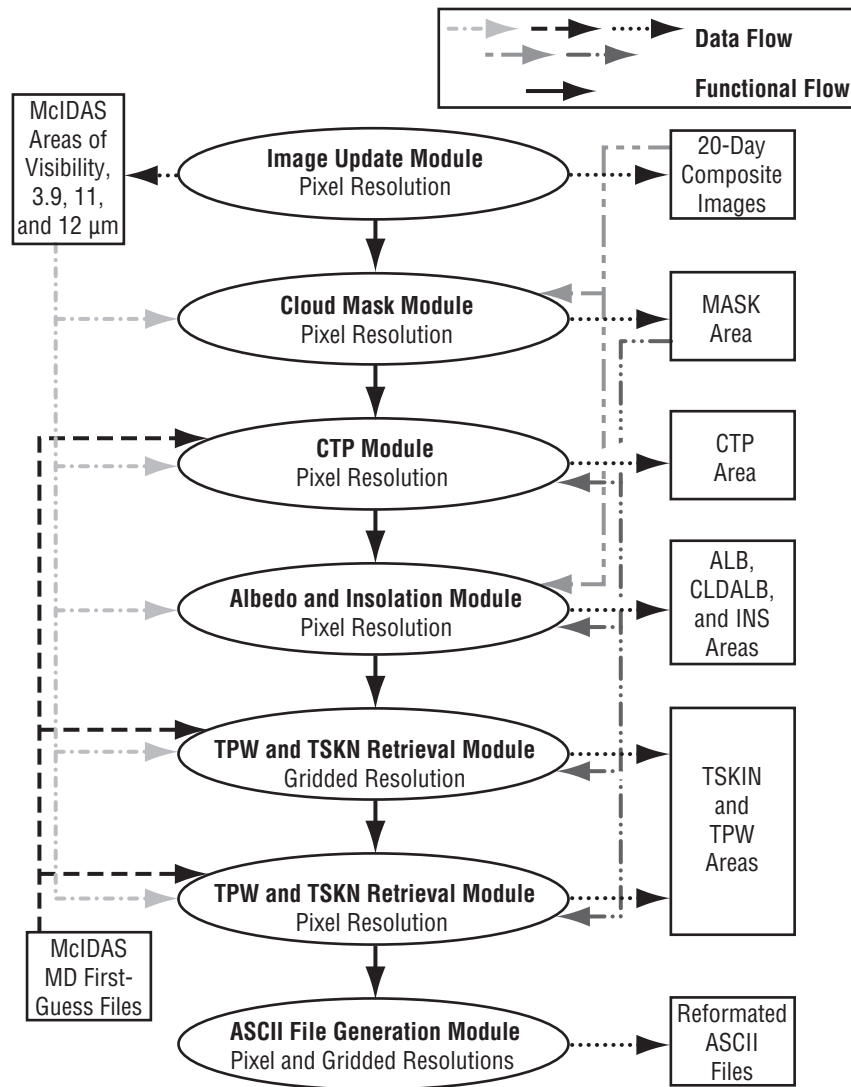


Figure 8. Diagram of the processing unit of GPGS.

Once the McIDAS areas of individual channels have been staged in a local data directory, the 20-day lists in the local directory of the visible, shortwave, and 11-μm longwave channels are updated. For each required channel, the most recent day is added to a 20-day list and the oldest day is deleted, then a single composite image based on minimum or maximum values from the 20 days is generated. For example, a minimum ALB image is generated from 20 days of visible data by comparing the ALB values for each pixel from the 20 days and retaining the minimum value. The purpose of this minimum ALB area is to provide clear-sky values to compare to the current visible image, thus there is an assumption that, for each pixel, at least 1 day within the 20 days will be cloud free and that the visible channel ALB values do not vary significantly within the time period.

Also generated is a maximum temperature 11- μm image using a similar method as described for the visible data, but the second warmest temperature is kept instead of the warmest. The reason for using the second warmest temperature is that it was found that using the warmest occasionally resulted in large differences between the maximum temperature values and the current 11- μm clear-sky values. The 11- μm surface temperature can vary significantly within a 20-day period with the passage of a front, and the assumption is that using the second warmest temperature will decrease the possibility of an extreme temperature being used while still obtaining a clear-sky value. Obviously this method is not error proof, but it is quick and simple and was found, over a several month study period, to provide better results than using the warmest temperature.

Additional 20-day composite images are generated from the difference between the 11- and 3.9- μm channels. Two minimum difference composite images are produced: (1) The smallest negative difference value is retained and (2) the smallest positive value. These two minimum difference images are generated for use by MASK, and their value will be explained in section 3.3.2.

In the real-time mode, the 20 days of images consist of the current day and the images from the previous 19 days or older if one or more images are missing for a particular time. In case-study mode there is more flexibility with the available data and the 20 days of images do not have to consist of the current day and the past 19 days. For example, for a 10-day case study, instead of generating different 20-day composite images for each day, a single set of composites for each hour can be generated using 10 days within the case study, the 5 previous days, and the 5 subsequent days. The goal of the composite images is to generate clear-sky values that are representative of the current conditions, and using surrounding days can therefore provide more accurate results.

3.3.2 Cloud Mask Module

A critical element in providing useful atmospheric and surface products is the ability to detect and monitor cloud cover on a 24-hr basis. The successful detection of clouds in day and night imagery eliminates cloud contamination in the TSKN and TPW products and provides a robust description of the clouds themselves in the CLDALB and CTP products.

3.3.2.1 Input and Output Data. The MASK module of GPGS requires the 11- μm longwave and the 3.9- μm shortwave images, the two 20-day composite images generated from the 11- μm minus 3.9- μm difference, and the 11- μm , 20-day maximum temperature composite image, which were all acquired or produced in the update image module. The MASK module generates a simple pixel resolution McIDAS area with values indicating cloud or no cloud. This output area is utilized by all of the succeeding modules in the processing unit of GPGS.

3.3.2.2 Algorithm Description. Guillory et al. presented a method for cloud detection using the shortwave and longwave window channels on the GOES Imager.⁹ Their method used single threshold values on brightness temperature and difference imagery to detect clouds at the pixel level. A modified version of this approach, called the bispectral spatial coherence (BSC) method, uses two spatial tests and one spectral threshold to identify clouds in the GOES Imager or Sounder imagery.¹⁰ The BSC technique was used operationally from 1998 to 2002 in the GPGS system. The performance of the BSC method was adequate during the day; however, poor performance of the algorithm at night prompted further changes to the algorithm. The new technique, called the bispectral threshold and height (BTH)

method, has been used in GPGS since 2002 and builds on the previous BSC method but adds spatial and temporal varying thresholds to the procedure.¹¹

An underlying principle of cloud detection using GOES imagery is that the difference between the emissivity of clouds at thermal wavelengths and at shortwave (reflective) wavelengths, such as 11 and 3.9 μm , respectively, varies from the same emissivity difference for the surface (land or ocean) and can be detected from channel brightness temperature, T_{bb} , differences. The emissivity at shortwave (SW), infrared wavelengths is less than at longwave (LW), infrared wavelengths for clouds, resulting in lower radiance values at the shorter wavelengths. During the day, reflected solar radiation makes the effective brightness temperatures (sum of emission and reflective components) at the shorter wavelengths larger than the brightness temperatures at the longer wavelengths even though the emissivity is less. Therefore, for cloudy pixels, $T_{bbLW} - T_{bbSW}$ has a large negative value during the day. At night, $T_{bbLW} - T_{bbSW}$ has a positive value (thick water clouds and fog) because there is no solar radiation or a negative value (thin cirrus) because, even though the emissivity of ice clouds is about the same for the two wavelengths, much of the sensed energy comes from Earth's surface and the 3.9- μm channel's response to warm subpixel temperatures is greater than it is at 10.7 μm . For noncloudy pixels, $T_{bbLW} - T_{bbSW}$ has a small (positive or negative) value during day and night. Thus, the transition from a clear to a cloudy region is manifested in the longwave minus shortwave brightness temperature difference image as a discontinuity. However, the fact that emissivities vary with cloud type and the effect of varying solar input at the surface or cloud top makes this a challenging problem.

The BTH technique uses multispectral channel differences to contrast clear and cloudy regions. The 11- and 3.9- μm channels are used to produce an hourly difference image (longwave minus shortwave) for this purpose. Positive differences, which mainly occur at low sun angles and at night, and negative differences, which occur at all times, are preserved in the difference image. Two composite images, which represent the smallest negative and smallest positive difference image values (values closest to zero) from the preceding 20-day period, are also created for each hour. These composite images serve to provide spatially and temporally varying thresholds for the BTH method. An additional 20-day composite image is generated for each hour using the second warmest longwave (11 μm) brightness temperature for each pixel from the 20-day period. This composite image is assumed to represent a warm, cloud-free thermal image for each time period.

The BTH method uses the above-mentioned image products in a four-step cloud detection procedure. This procedure is schematically described in figure 9. All of the threshold values listed are subject to change, and the values may differ between the Imager and Sounder MASKs because of the differences in wavelengths of the channels of the two instruments. The first step of the MASK algorithm subjects each pixel in the difference image (DI) to an adjacent pixel test. The variance between pixels $DI(i)$ and $DI(i-1)$ along the scan line in the difference image is computed. If the variance between these adjacent pixels is >7.25 K, a cloud edge is detected. This procedure is more successful in identifying the edges of many clouds during the day than at night. The second step attempts to fill in between the cloud edges by analyzing the one-dimensional spatial variability of the pixels. The difference between $DI(i)$ and $DI(i-1)$ is calculated. For a cloud to be detected, this calculated difference value must be <0 K if the preceding image location ($i-1$) was cloudy, or it must be less than -3 K or >2 K if the preceding image location was clear. In this way the spatial variability in the difference image corresponding to a cloud-free surface versus a cloud is considered.

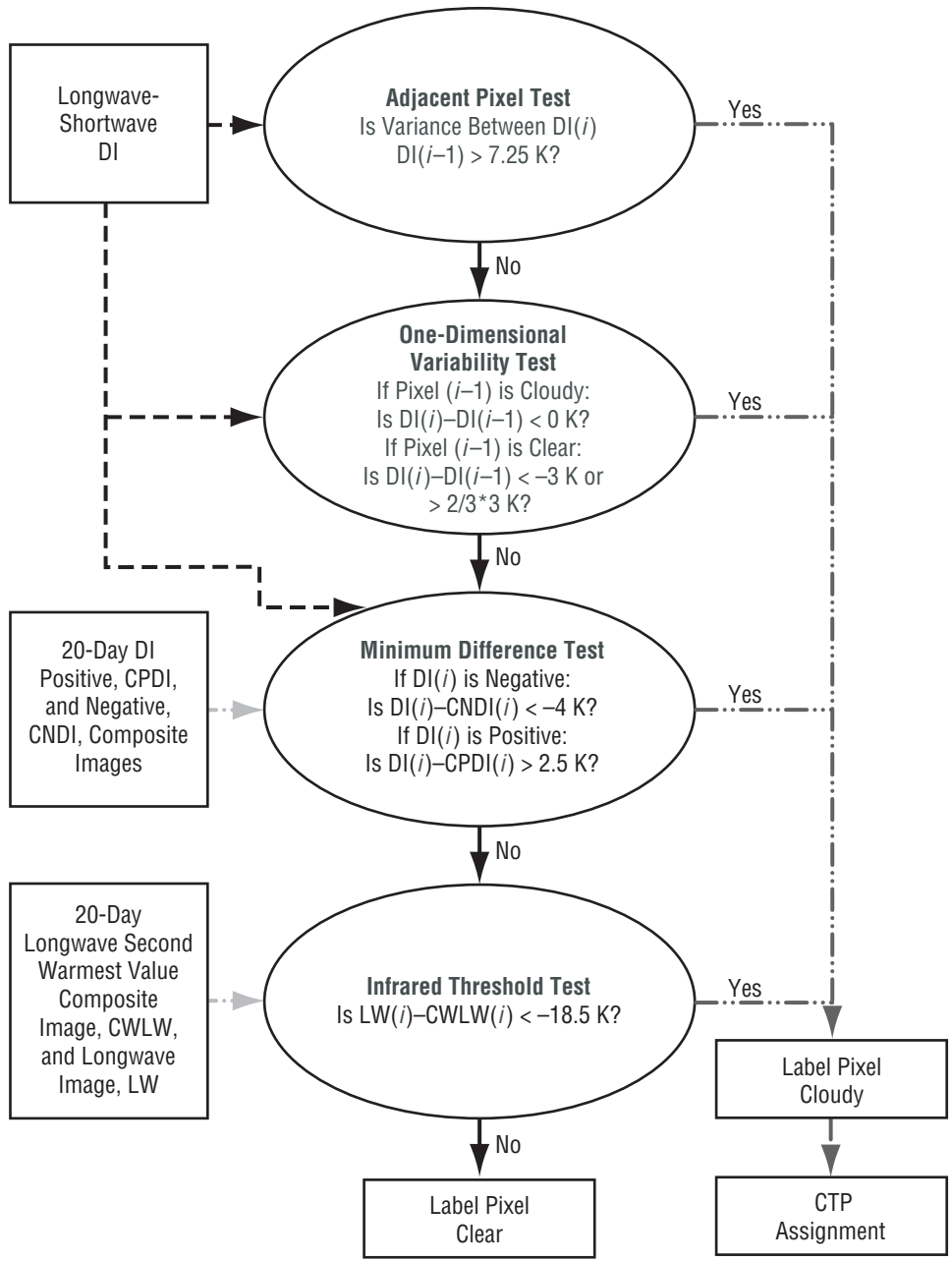


Figure 9. Diagram of the BTH cloud algorithm.

The third step in the BTH method detects clouds using a minimum difference test in regions where the first two steps fail. This step utilizes the positive and negative composite images derived for each hour, which, respectively, represent the smallest positive and negative difference image values from the preceding 20-day period. The minimum difference test compares the current difference image value to these composite images. A pixel is deemed cloudy if the difference between $DI(i)$ and the smallest positive value is >2.5 K or if the difference between $DI(i)$ and the smallest negative value is less than -4 K. The 20-day composite positive and negative difference images incorporate spatially varying infor-

mation for nighttime and daytime cloud determinations separately. This is a significant change from the previous BSC method, which did not separate positive and negative differences.

The fourth and final step in the BTH method involves using the longwave channel information and catches a few clouds missed by the previous three tests. This infrared threshold test uses an hourly 20-day composite of the second warmest thermal infrared channel values at each pixel location. This product is essentially a warm, cloud-free thermal infrared image. A pixel in the observed infrared image is deemed cloudy if it is 18.5 K colder than the warm thermal infrared channel composite image for that location and time period.

3.3.2.3 Validation. Jedlovec and Laws have shown that the BTH algorithm is substantially better than its predecessor, the BSC method.¹¹ In their assessment, a comparison was made of the BTH and BSC automated cloud detection methods with subjectively determined cloud or no-cloud conditions at various times of the day during four 2-wk-long case studies, each corresponding to a different season. The new; i.e., BTH, algorithm greatly improves cloud detection near sunrise and sunset and at night. The underdetermination of clouds (cloud pixels not properly identified) by the earlier BSC technique was substantially reduced with the new method, even at night, with just a few percent of the clouds going undetected. The correct determination of cloudy and clear pixels occurred >90 percent of the time in the study when all seasons and times were considered.¹¹

Examples of the GPGS MASK and CTP product are shown in figures 10 and 11. MASK is color coded to indicate which test detected the cloud—with the pixel colored white if more than one test detected the cloud. Note that the minimum difference test is split into positive and negative difference tests. The color key for MASK for figures 10 and 11 is provided in figure 10. Figure 10 provides a daytime example and is shown along with the corresponding visible and infrared imagery. Notice that MASK detects almost all the clouds and does not significantly overdetermine. The CTP product distinguishes between high and low clouds that appear the same in the visible imagery, such as over North Carolina. Figure 11 provides a nighttime example together with the infrared imagery. Notice that the nighttime example does not detect as high a portion of the clouds as the daytime example, but does detect clouds that are not easily seen in the imagery, such as over southern Georgia. Also notice that there are more clouds detected by only one test, with a significant portion being detected by only the positive difference test.

3.3.3 Cloud Top Pressure Assignment Module

The vertical distribution of CTP or height over a geographical region is useful information in weather analysis and modeling studies. In the GPGS system, a CTP is assigned to each pixel that is determined to be cloudy in the GOES imagery. The clouds are assumed to be uniform in coverage and height over the GOES pixel. The GPGS CTP module requires the first-guess MD files generated in the preprocessing unit and the 11- μm and MASK McIDAS areas. The pressure assignment is similar to that used by Fritz and Winston and applied by Jedlovec et al.^{12,13} A forecast temperature field valid at the cloud observation time from the MM5 regional model run in real time at GHCC is used. The GOES 11- μm window channel (of either the Imager or the Sounder) brightness temperature corresponding to each cloudy pixel is referenced to the closest thermodynamic profile corresponding in the model grid point data. No attempt is made to correct the brightness temperature for the affect of water vapor above the cloud. Log-linear interpolation is used between model vertical pressure levels to assign a pressure corresponding to the cloud top temperature.

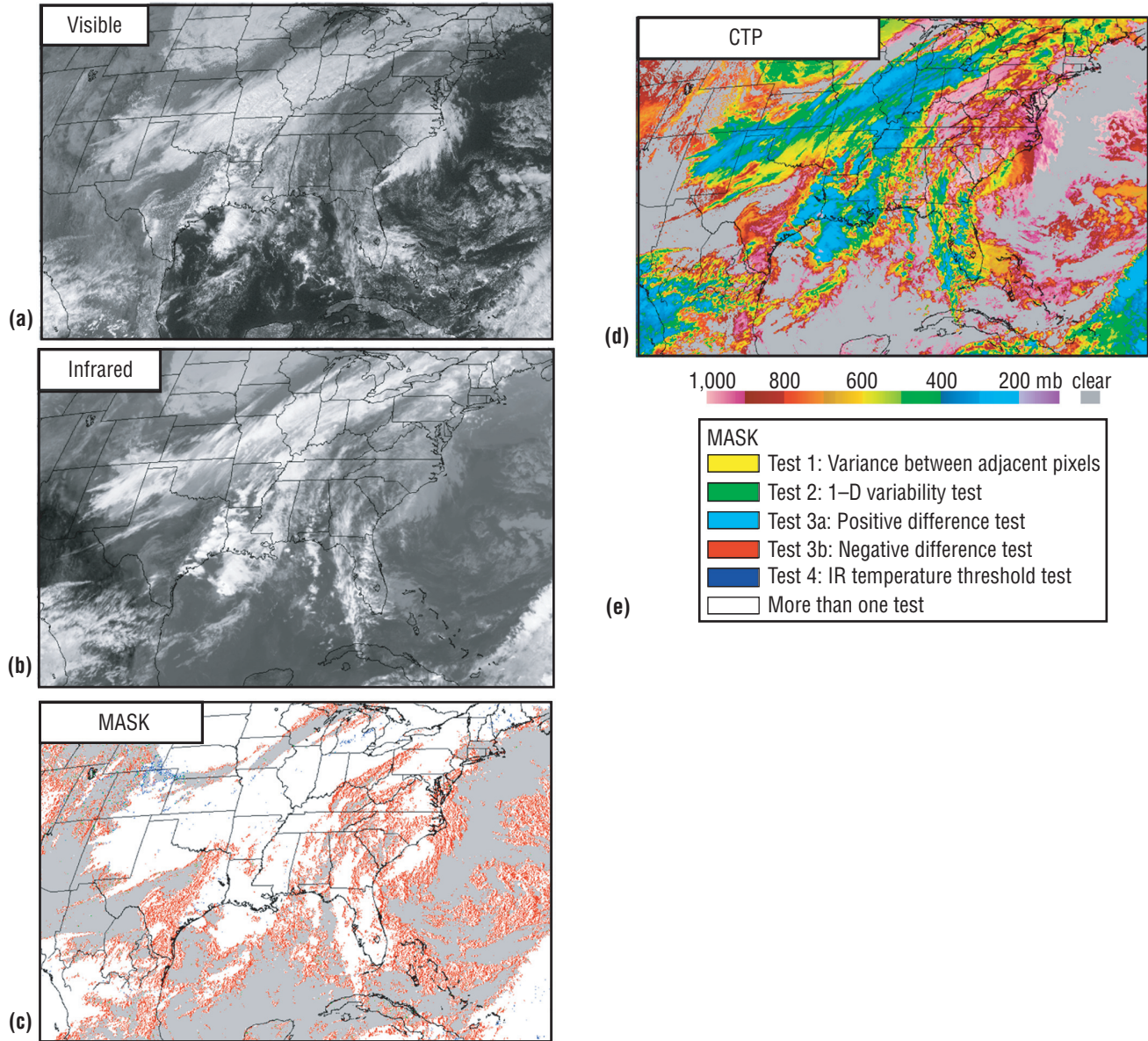


Figure 10. Daytime (1845 UTC, October 25, 2003) example of the (a) visible and (b) infrared imagery, the GPGS (c) MASK and (d) CTP product, for the same time, and (e) the color key for the MASK image.

The approach works well for opaque clouds where the cloud emissivity is close to unity and emission (measured by the satellite) comes primarily from the cloud top. The quality of CTP retrievals are dependent on the radiometric accuracy of the satellite data (window channel data), the accuracy of the temperature profile from the model, and the amount of water vapor above the cloud. Typical pressure assignment errors are on the order of 25–50 mb (for an 11- μm root mean square (RMS) error (RMSE) of 0.5 K and a 2 K forecast error). For nonopaque clouds, such as thin cirrus, emission from below the clouds is detected by the satellite and cannot be separated from cloud emission without knowledge of

the cloud emissivity, which results in CTPs that are too large. The affect of water vapor on the window channel brightness temperature could produce ≈ 25 mb bias in the heights. This bias would be greatest for low clouds and would result in clouds having assigned pressures that are too low in magnitude.

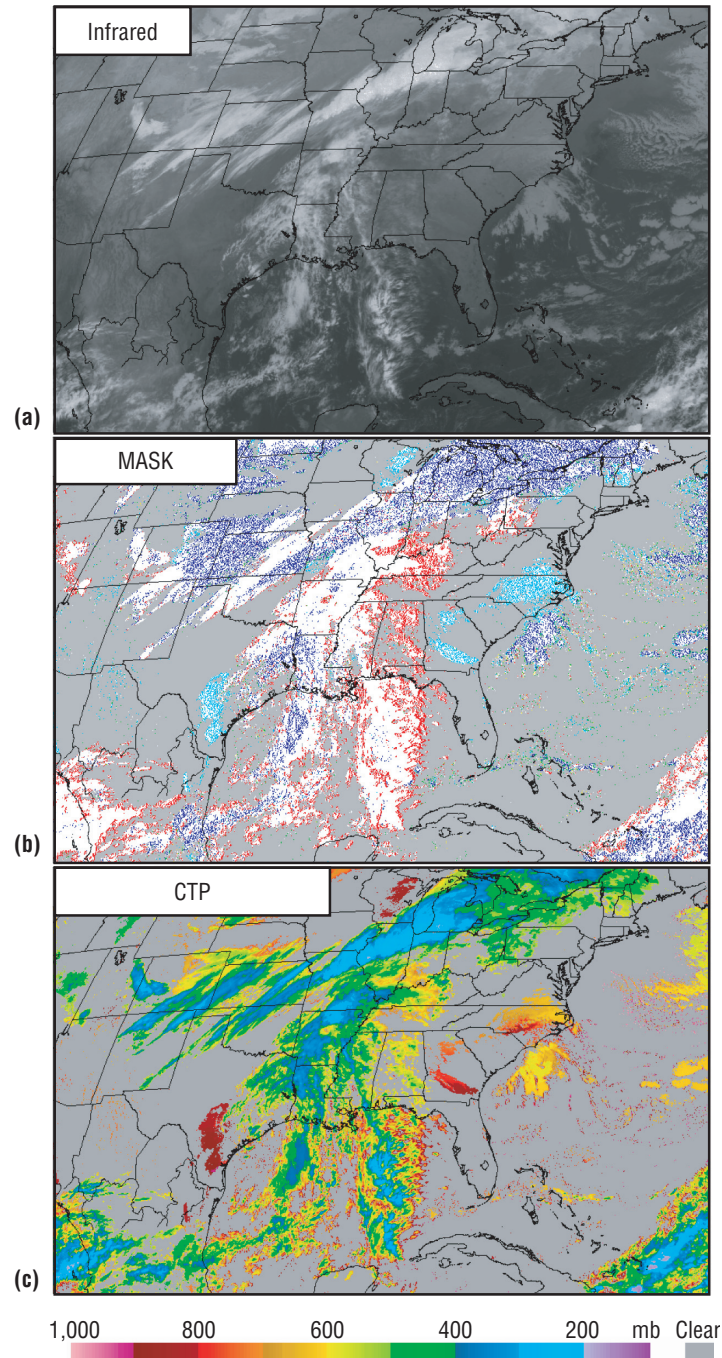


Figure 11. Nighttime (0845 UTC, October 15, 2003) example of the (a) infrared imagery and the GPGS (b) MASK and (c) CTP product. See figure 10 for the MASK color key.

3.3.4 Albedo and Insolation Module

The ALB and INS module is a McIDAS-based Fortran program consisting of file input and output logic and an algorithm for calculating ALB, CLDALB, and INS. The module consists of a McIDAS-based Fortran program incorporating an algorithm that is an implementation of the Gautier et al. method with improvements from Diak and Gautier.^{14,15} The Gautier approach is a physical method to calculate incident and net solar radiation at the surface, based on energy conservation principles using measurements from the visible channel of GOES. ALB is calculated by using a visible 20-day clear-sky composite image, which is generated in the image update module. CLDALB is calculated from the current visible-channel measurement along with the knowledge of the ALB. INS is determined as the sum of solar radiation incident at the surface from both direct and diffuse sources, taking into account the effects of atmospheric absorption and scattering and the attenuation by clouds.

3.3.4.1 Input and Output Data. The ALB and INS module requires the clear-sky composite and the current visible-channel McIDAS areas. The algorithm requires that the input be in units of radiance, W/m^2 . Thus, when the data are read from the areas within the program, either McIDAS calibration is applied to the raw satellite measurements or an option is available to apply a manual calibration to convert the raw values to radiances. The manual calibration is defined in the program using calibration coefficients associated with detector 2 of the GOES Imager instrument. At the time of this writing, the code had not been modified for the Sounder instrument. Note that McIDAS internal calibration does not use detector 2 coefficients, thus differences between the calibration methods are seen in the ALB and INS values. An additional option is also available to correct for the GOES-8 Imager visible-channel detector degradation drift. The comparison of GOES-8 visible-channel scenes over time has indicated a detector degradation resulting in a decrease in scene radiance of ≈ 6 percent/yr.^{16,17} Correction values for additional satellites will be included as the degradation results are made known. Figure 12 shows examples of the three products of the ALB and INS module derived from GOES-8 Imager data with and without the correction of the degradation of the visible channel.

The output files of the ALB and INS module are McIDAS files of ALB, CLDALB, and INS at pixel resolution. The ALB files contain values with units of percentage multiplied by 10. The unit for the INS area is W/m^2 , with no scaling.

3.3.4.2 Algorithm Description. The ALB and INS algorithm, using Gautier's approach, employs a clear and a cloudy atmosphere model applying the effects of Rayleigh scattering, ozone absorption, water vapor absorption, and cloud absorption and reflection. The effects of Rayleigh scattering are modeled after Coulson and Allen for the GOES-8 visible band radiant flux viewed by the satellite and for the bulk solar flux incident at the surface.^{18,19} Ozone absorption is modeled after Lacis and Hansen in the GOES visible band and in the total solar flux.²⁰ Water-vapor absorption is assumed to be negligible in the ALB and CLDALB calculation involving the radiance in the GOES visible band, but it is accounted for when applying the total solar flux in the INS calculation. Water-vapor absorption coefficients are obtained from Paltridge, and total column water vapor is assumed to be 25 mm and adjusted for solar zenith angle.²¹ Cloud absorption is modeled as a constant of 7 percent of the incident flux at the top of the cloud.

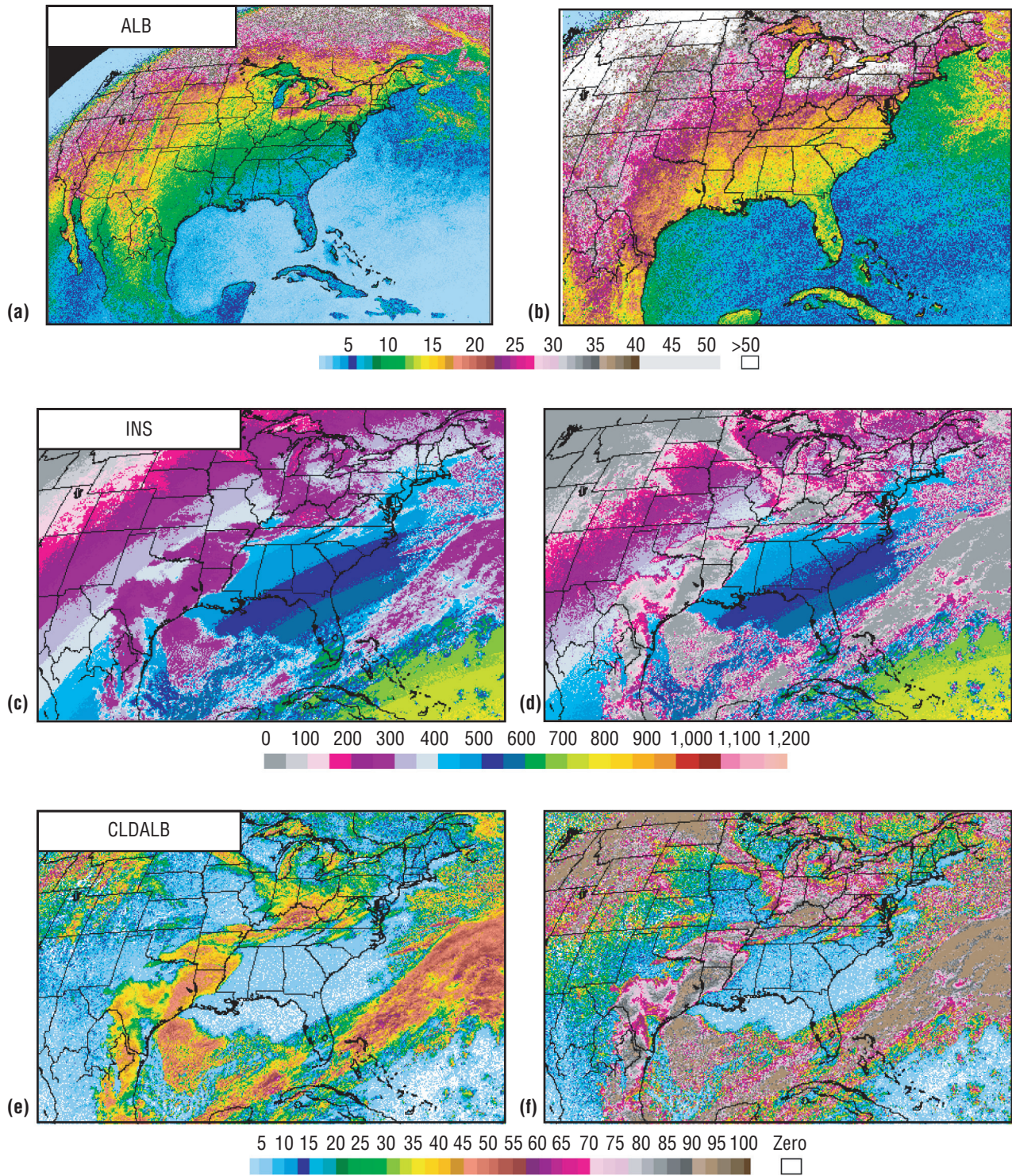


Figure 12. Examples of GOES-8 (a) uncorrected and (b) visible channel degradation corrected ALB (%), (c) uncorrected and (d) corrected INS (W/m^2), and (e) uncorrected and (f) corrected CLDALB (%) at 1545 UTC, January 14, 2003.

In the Gautier method, ALB is first calculated for the entire scene, clear or cloudy, by using the clear-sky composite image. This is done by formulating the physical processes that describe the radiant energy observed at the satellite as a function of the incident solar energy at the top of the atmosphere and the planetary ALB, which includes surface reflection. This radiation transfer formulation can then be set equal to the radiance measured at the satellite. Since the absorption and scattering processes described above are estimated, the radiation equation can be solved for the only unknown, which is ALB. The ALB values are considered valid for the current scene, whether clouds are present or not.

For the clear-sky case, the incident shortwave radiation at the surface can be formulated as the sum of two terms: (1) The incident solar flux that is attenuated by Rayleigh scattering, ozone, and water vapor absorption, and (2) the surface reflected flux that is scattered back to the surface by Rayleigh scattering. With ALB known and the absorption and scattering processes estimated, INS can be calculated directly.

The cloudy-sky model is similar to the clear-sky case, except it uses CLDALB. CLDALB is calculated in a manner similar to the calculation of ALB, except it involves cloud processes. The radiance at the satellite is formulated as a function of the incident solar flux involving four processes: (1) Atmosphere backscatter, (2) the reflection from the cloud surface, (3) a component of the cloud reflected energy that is backscattered to the cloud by Rayleigh scattering and then to the satellite, and (4) a component passing through the cloud, reflected from the surface, and back through the cloud to the satellite. Since the radiance at the satellite and ALB are known, along with estimates of the scattering and absorption processes, the radiation formulation can be solved for the CLDALB. The input current GOES visible-channel image is used as the measurement of the radiance at the satellite for the CLDALB calculation. Knowledge of the CLDALB allows for the calculation of the cloudy-sky INS. This is formulated as the sum of the incident solar flux attenuated by scattering and absorption processes, including cloud absorption, and surface reflection that is backscattered from the cloud to the surface.

In practice, the algorithm calculates INS using both the clear-sky and cloudy-sky formulations for a given scene. If the cloudy-sky calculation is greater than or equal to the clear-sky value, then the clear-sky value is used and the scene is assumed clear. This is consistent with the CLDALB being near zero for clear-sky conditions. In cloudy conditions, the bulk solar cloud absorption of 7 percent of the incident flux at the cloud top is assumed for thick clouds. Since the effect of CLDALB dominates in the INS calculation, uncertainties in cloud thickness have been shown to produce only small effects on the INS calculation.

Since scattering and absorption processes do not include aerosols, the presence of aerosols is expected to affect the calculation of the INS values. For the case when the presence of aerosols does not indicate cloudy conditions, the resulting INS will be in error. Though the signal in the net shortwave energy budget at the surface is expected to be in the direction of the actual value, the magnitude will be in question. In the case of smoke; e.g., burning biomass, the algorithm will discern the smoke as a cloud if its areal extent is larger than the resolution of the sensor. Cloud absorption and scattering properties will be applied in this case. The effect is estimated to produce a signal in the INS value in the direction of the actual value; however; its accuracy will be in question.

3.3.4.3 Validation. There has been no intensive validation of the GPGS ALB and INS products, but several comparisons of INS to surface measurements have shown fairly good agreement. The surface

measurements were obtained from a Surface Radiation Budget Network (SURFRAD) location in Northern Mississippi.²² The SURFRAD sites provide measurements of the surface radiation budget over the United States. For comparisons to the satellite-derived INS product, a total solar irradiance value was computed from the SURFRAD measurements. The total is the sum of the direct solar radiation and the radiation scattered (diffuse), with the direct first being multiplied by the cosine of the solar zenith angle because the direct measurement is made normal to the Sun's beam and the direct amount that is falling on a horizontal surface is needed. The SURFRAD measurements have been found to be within 15 W/m² of standard measurements for almost all cases.²²

The charts in figure 13 provide examples of clear- and cloudy-sky comparisons between the SURFRAD measurements and GOES-8 (fig. 13) and GOES-12 (fig. 14) Imager INS-derived values. For the GOES-8 examples, INS retrieval values are provided that were derived using visible-channel ALB values that were corrected for the degradation and those that were not corrected. During clear-sky conditions, the correction of the visible channel does not have a significant effect, and both of the GOES INS values are higher than the SURFRAD values for all hours, with the largest differences occurring midday. The visible-channel correction has a significant effect under cloudy conditions, as seen in the March 1, 2003, example. The GOES-8 Imager INS values without the correction are significantly higher than the SURFRAD values, but the GOES values using the corrected visible data show good agreement to the SURFRAD data, except during the 1645–1745 UTC time period when the satellite retrievals are too low with respect to the ground measurements.

The GOES-12 INS retrievals are currently made without any correction to the visible channel since GOES-12 is a new satellite and degradation of the visible channel has not yet become significant. The clear-sky comparison for the September 15, 2003, example shows very good agreement between the satellite and ground measurements. The April 24, 2003, cloudy example also shows very good agreement.

Direct validation of the ALB and CLDALB products has not been done. However, since the INS calculation is dependent on the ALB value, indirect validation of these quantities may be assumed when validating the INS retrievals. This may be especially true in the cloudy-sky case where CLDALB significantly affects the amount of energy reaching the surface.

3.3.5 Skin Temperature and Total Precipitable Water Retrieval Module

TSKN is the radiating temperature of the soil, vegetation, top of canopy, buildings, roads, water, etc. TPW is the total amount of water vapor contained in a vertical column of a unit of cross-sectional area extending from the surface to the top of the atmosphere. TSKN and TPW can be retrieved simultaneously using a physical split-window technique that utilizes two channels that are within the same atmospheric window; i.e., a region of the electromagnetic spectrum where atmospheric absorption of radiation is at a minimum. Upwelling radiation from the surface in the 10- to 12.5- μm atmospheric window is partially absorbed by water vapor in the atmosphere. To correct for the absorption of the upwelling radiation and obtain the true emission from the surface, two channels within the same window are used. For the 11- μm window channels of the Imager and Sounder, the atmospheric absorption is small, and thus, a significant portion of the radiation signal received by the satellite is from the surface. For the 12- μm channels, additional water-vapor absorption reduces the atmospheric transmittance, and for this reason, the 12- μm channels are sometimes referred to as dirty channels. By utilizing two channels with similar wavelengths, the difference between the two channels is assumed to be the result of the differential

absorption of water vapor in the atmosphere. Thus, the atmospheric absorption component can be determined and the TSKN and TPW values can be simultaneously retrieved.

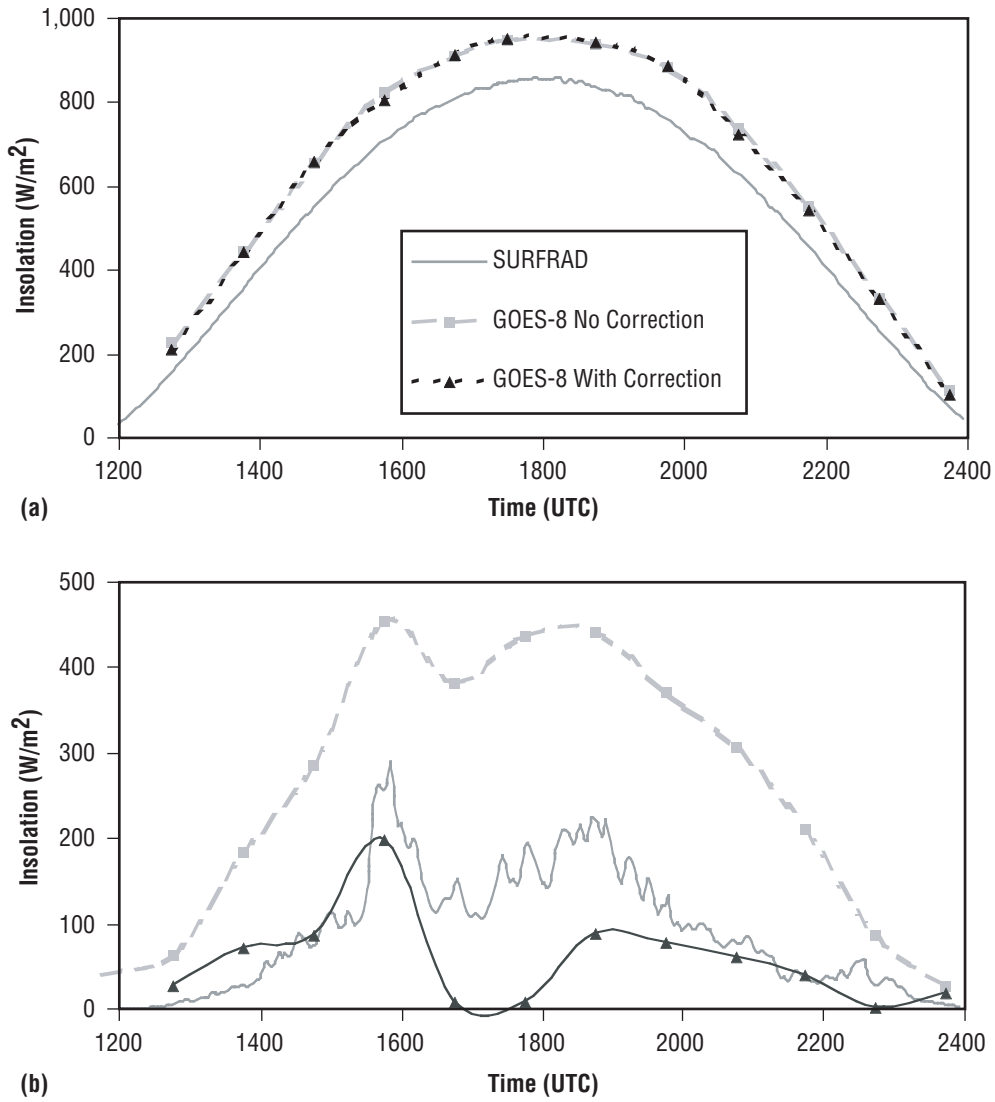


Figure 13. GOES-8 INS retrievals compared to SURFRAD measurements for (a) the August 29, 2000, INS and (b) the March 1, 2003, INS at Goodwin Creek, MS.

TSKN and TPW products are retrieved by GPGS for all the clear pixels as determined by MASK by a McIDAS-based Fortran program known as GOESRET that uses a physical infrared split-window retrieval algorithm developed by Jedlovec.²³ GOESRET has many input and output parameters and options that control aspects of the retrievals, such as the execution mode or batch mode for GPGS. Different retrieval location and resolution strategies are also available as options. Retrievals can be performed at the input guess profile locations, specific latitudinal and longitudinal locations, such as on a

model grid, and at each pixel location. When the resolution of the output retrievals is coarser than pixel resolution or when smoothing of the retrievals is desired, the input infrared radiances are averaged, not the output retrievals. For locations, or footprints, consisting of averaged pixels, retrievals are made, provided the number of clear pixels within each footprint exceeds the specified minimum percentage. Typically, 66 percent of pixels are required to be clear for a retrieval to be made, or else the location is labeled as cloudy. When averaging occurs and the location has been determined to be clear, only clear pixel radiances are included in the averaging.

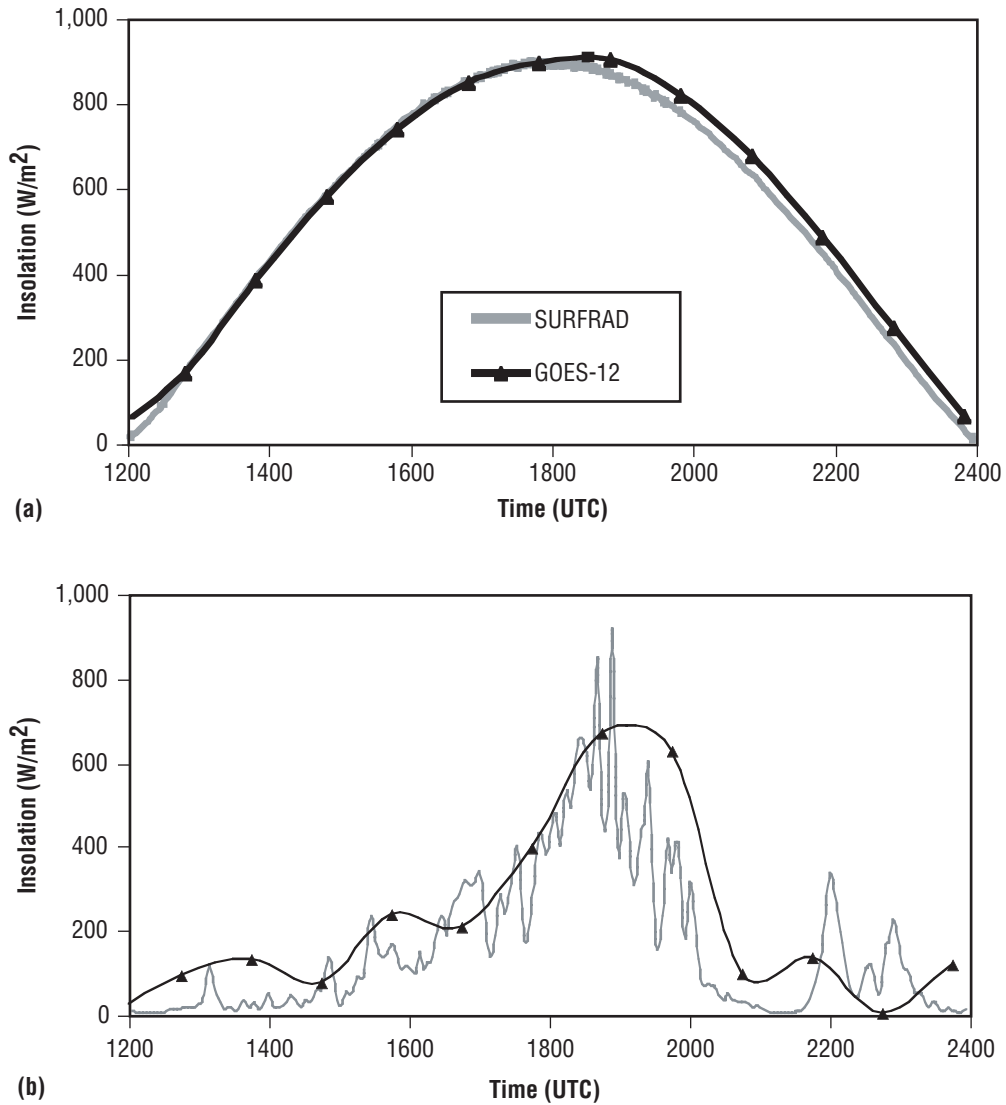


Figure 14. GOES-12 INS retrievals compared to SURFRAD measurements for (a) the September 15, 2003, INS and (b) the April 24, 2003, INS at Goodwin Creek, MS.

3.3.5.1 Input and Output Data. Inputs for GOESRET are in the form of control parameters and data files. The control parameters are read by GOESRET by command line inputs. Control parameters specify which options and thresholds to employ during execution. Input and output file options are also specified by command line inputs.

GOESRET requires the input of at least two McIDAS areas containing radiance measurements from the GOES longwave infrared window region (10.5–12.5 μm), and the MASK area generated previously in the processing section of the GPGS. The first-guess file generated in the preprocessing section is also required. The profiles of temperature and precipitable water at pressure levels within the first-guess MD file are assumed to be valid for a time and location near that of the retrieval. Recall that the first-guess file also contains additional profiles of precipitable water set to 80 percent of the original values and associated perturbed transmittances. These perturbed quantities are used to approximate the derivative of transmittance with respect to precipitable water, which is used by the retrieval algorithm described in section 3.3.5.2.

Depending on the retrieval location and resolution strategy, two additional files may also be needed. These files are a retrieval location file and a guess grid navigation information file. The retrieval location file is an ASCII file containing latitudes and longitudes of the retrieval locations. The navigation file contains information about the guess grid projection parameters. GOESRET uses these navigation parameters to determine the closest guess grid to the retrieval location.

Several data file output options are available. These output options include the McIDAS MD file, McIDAS area file, and ASCII file. Data written to an MD file not only include the retrieved parameters but also auxiliary data for diagnostic evaluation of the algorithm execution. MD files are mainly used internally for research and retrieval performance evaluations. TSKN and TPW retrievals can also be written to McIDAS area files, although this option is only available when the retrieval spatial resolution is at the pixel interval. The ASCII file option provides a formatted file not only containing TSKN and TPW values, but also latitudinal and longitudinal locations, cloud flags, and retrieval status information. The ASCII file is the primary GOESRET output used in creating data product files for distribution to users of the data, such as for model assimilation. The units for the retrieved TSKN and TPW are degrees Kelvin and millimeters of water, respectively.

3.3.5.2 Algorithm Description. The GOESRET retrieval algorithm is an implementation of a perturbation solution of the radiative transfer equation to obtain TSKN and TPW. The basic algorithm was first developed by Jedlovec and subsequently evaluated by Guillory et al. and Suggs et al.^{23–25} The algorithm requires at least two longwave infrared window channel observations to simultaneously solve for perturbations or departures of TPW and TSKN from guess values of these quantities. Additional input guess values required by the algorithm include profile estimates of temperature, precipitable water, and channel transmittance for the observed scene. Also, a perturbed profile of precipitable water and corresponding channel transmittance is needed. From these profiles, coefficients are calculated that are used in solving the perturbation equation for the perturbations of TSKN and TPW.

The radiative transfer equation describing the upwelling radiation, I , observed at the satellite, assuming a nonscattering plane parallel atmosphere, can be expressed as

$$I = \varepsilon B(T_s) \tau_{ps} + \int_{ps}^0 B[T(p)] \frac{\partial \tau(p)}{\partial p} dp + (1 \pm \varepsilon) \int_{ps}^0 B[T(p)] \frac{\tau_{ps}^2}{\tau(p)^2} \frac{\partial \tau(p)}{\partial p} dp \quad , \quad (1)$$

where τ and B are the transmittance and Planck function, respectively, for a wavelength domain associated with an infrared sensor window channel. The quantities T , T_s , and p are the temperature, TSKN, and pressure, respectively, and the subscript “ ps ” denotes that the atmospheric parameter is evaluated at the surface pressure. The quantity ε is the emissivity. The perturbation equation is obtained by substituting the quantities

$$T_s = \bar{T}_s + \delta T_s \quad , \quad (2)$$

$$\tau = \bar{\tau} + \delta \tau \quad , \quad (3)$$

and the approximation

$$\delta \tau \approx \frac{\partial \bar{\tau}}{\partial U} \delta U \quad (4)$$

into the first two terms of the right-hand side of equation (1), where the over-bar denotes a guess quantity, δ denotes a perturbation from the guess value, and U is a precipitable water. Thus, \bar{T}_{ps} is the guess surface air temperature while \bar{T}_s is the guess TSKN. In addition, four assumptions are made: (1) The perturbation contribution from the reflective term in equation (1), the third term on the right-hand side, is assumed to be small and ignored; (2) the guess moisture profile has the same structure as the actual moisture profile yielding the relationship

$$\frac{\delta U(p)}{\bar{U}(p)} \approx \frac{\delta U_{ps}}{\bar{U}_{ps}} = \text{constant} \quad ; \quad (5)$$

(3) the guess air temperature profile is very close to the actual temperature profile; and (4) the guess profiles have the same atmospheric depth as the actual retrieval location; i.e., the terrain has the same elevation height.

The resulting perturbation equation for each channel observation is given by

$$\delta I = C \delta T_s + D \delta U_{ps} \quad , \quad (6)$$

where δI is the difference between the radiance observed by the satellite and the radiance calculated using equation (1) with the guess temperature, moisture, and transmittance profiles representing the observed scene. The coefficients C and D are defined as

$$C = \varepsilon \tau_{ps} \frac{\partial B(\bar{T}_s)}{\partial T} \quad (7)$$

and

$$D = \frac{\partial \bar{\tau}_{ps}}{\partial U} [\epsilon B(\bar{T}_s) - B(\bar{T}_{ps})] - \frac{1}{\bar{U}_{ps}} \int_{ps}^0 \bar{U}(p) \frac{\partial \bar{\tau}(p)}{\partial U} \frac{\partial B[\bar{T}(p)]}{\partial p} dp \quad . \quad (8)$$

The retrieved TSKN, T_s , and TPW, U_{ps} , are obtained by applying equation (6) for two or more sensor channels in a matrix formulation to solve for the perturbations δT_s and δU_{ps} . TSKN and TPW are then obtained from the definitions given in equation (2) and

$$U_{ps} = \bar{U}_{ps} + \delta U_{ps} \quad . \quad (9)$$

A more detailed derivation of the perturbation equation (eq. (6)) using this approach is given by Suggs et al.²⁵

For quality retrievals of TSKN and TPW, the guess profiles of temperature and precipitable water must be consistent with the assumptions or constraints listed above. In addition, it is assumed that the derivative of transmittance with respect to precipitable water, $\partial \bar{\tau} / \partial U$, in equation (8) is sufficiently approximated by the ratio $\Delta \bar{\tau} / \Delta \bar{U}$ obtained from the difference between the guess transmittance profiles and transmittances calculated from a perturbed guess precipitable water profile. The perturbed precipitable water profile is usually taken to be 80 percent of the guess profile. The guess moisture and transmittance profiles also need to take into account the view angle between the satellite and the retrieval location. In application, guess profile preparation including satellite view angle and the transmittance calculations are performed outside the algorithm, and thus the guess profiles are inputs to the GOESRET program.

The condition requiring that the guess profiles have the same terrain elevation as the retrieval location is, in many cases, difficult to meet. The resolution of the guess field may not be fine enough to characterize the terrain variability. In order to improve retrieval performance when there is a significant difference between the first-guess and retrieval resolutions, the algorithm can use a terrain database to adjust the surface level of the guess profiles. The terrain database can also be an input to the GOESRET program.

3.3.5.3 Validation. As part of GPGS, the GOESRET algorithm has been producing TSKN and TPW products daily, on an hourly basis, initially from GOES-8 Imager and Sounder and most recently from the GOES-12 Sounder. During this time, several case studies have been performed to assess the performance of the algorithm, determine the quality of the retrieved parameters impacted by instrument noise and resolution, and evaluate the utility of assimilating the time rate of change (tendency) of retrieved TSKN into the MM5 to improve forecasts. Presented below are several examples of analyses that have been performed.

The performance of the GOESRET algorithm was evaluated by Suggs et al. by applying the algorithm in a simulated GOES measurement case study.²⁵ Hourly GOES-8 radiances were simulated by applying GOES-8 channel response functions and an appropriate radiative transfer code to TSKNs and atmospheric profiles of pressure, temperature, and moisture obtained from a mesoscale model run. The model run provided hourly data over a 12-hr period for June 17, 1986, at 35-km resolution over the eastern Central United States. The simulated radiances were at the same resolution as the model data

and contained no instrument noise or calibration error characteristics. The GOESRET algorithm was applied to the simulated radiances by performing retrievals at each hour and at the same resolution as the measurements. The retrieved TSKN and TPW were then compared with those from the model run at the retrieval location from which the radiances were calculated in order to obtain retrieval error statistics. Thus, the model run served as ground truth for the retrieved values. This type of case study is useful in evaluating the sensitivity of the retrieval algorithm to various retrieval conditions and input control parameters, such as the first-guess field. Since the simulated measurements (radiances) did not include error effects, such as instrument noise and biases and radiative transfer code inadequacies, the retrieval error statistics represent a lower boundary on the expected accuracy of the algorithm when applied in a real-world setting.

The first-guess field used in the case study was obtained from the model run, the same model run from which the radiances were produced. However, in order to provide a realistic first-guess field, the quality of the first-guess field was degraded by using the model profiles at a greatly reduced resolution of ≈ 250 km; moreover, the guess TSKN was assigned the surface air temperature of the model profiles. In order to assess the quality of the first-guess field, the first-guess TPW and TSKN used in the retrieval were compared to the model values at the retrieval locations (ground truth). Statistics were calculated from these comparisons and are herein referred to as the first-guess error. Thus, GOESRET algorithm performance can be evaluated by comparing the retrieval error with the first-guess error, thereby, providing the amount of improvement the algorithm retrieval provides over the first-guess value.

The results of the case study indicated that the retrieved TPW error is very sensitive to the quality of the first-guess field while the TSKN error is only slightly sensitive (figs. 15 and 16, respectively). The results also show that the algorithm's TPW performance had a diurnal effect while the TSKN performance did not. Statistics of one of the TPW analyses from Suggs et al. demonstrating these results are presented in figure 15.²⁵ It is seen that the mean TPW retrieval error (fig. 15(a)) and the TPW first-guess error are near zero, thus indicating that there is very little bias in the first-guess or retrieved TPW. However, the standard deviation (SD) of the TPW retrieval error (fig. 15(b)) is seen to vary significantly with respect to time of day while the guess TPW SD is fairly constant. During the late morning and afternoon hours, the TPW retrievals show an improvement over the guess value, but during the night the TPW retrieval degrades and becomes worse than the guess TPW. Suggs et al. show that the cause for the nighttime degradation in the TPW retrievals appears to be due to temperature inversions at the surface.²⁵ For TSKNs cooler than the near-surface air temperature, the coefficient associated with the TPW perturbation in the perturbation equation (eq. (6)) tends toward zero. This causes the magnitude of that term to become similar to the values of the approximations made in the linearization of equation (6). Other analyses performed by Suggs et al. show that the TPW error increases when the first-guess error is also increased.²⁵ Moreover, the TPW retrieval demonstrates a bias when there is a similar bias in the TPW first-guess. For this study, only two channels were used in the retrieval algorithm; i.e., GOES-8 Imager application. Analysis has not been performed to determine if the above results are obtained when more than two spectral channels are used by the algorithm. Additional channels are available on the GOES Sounder instrument.

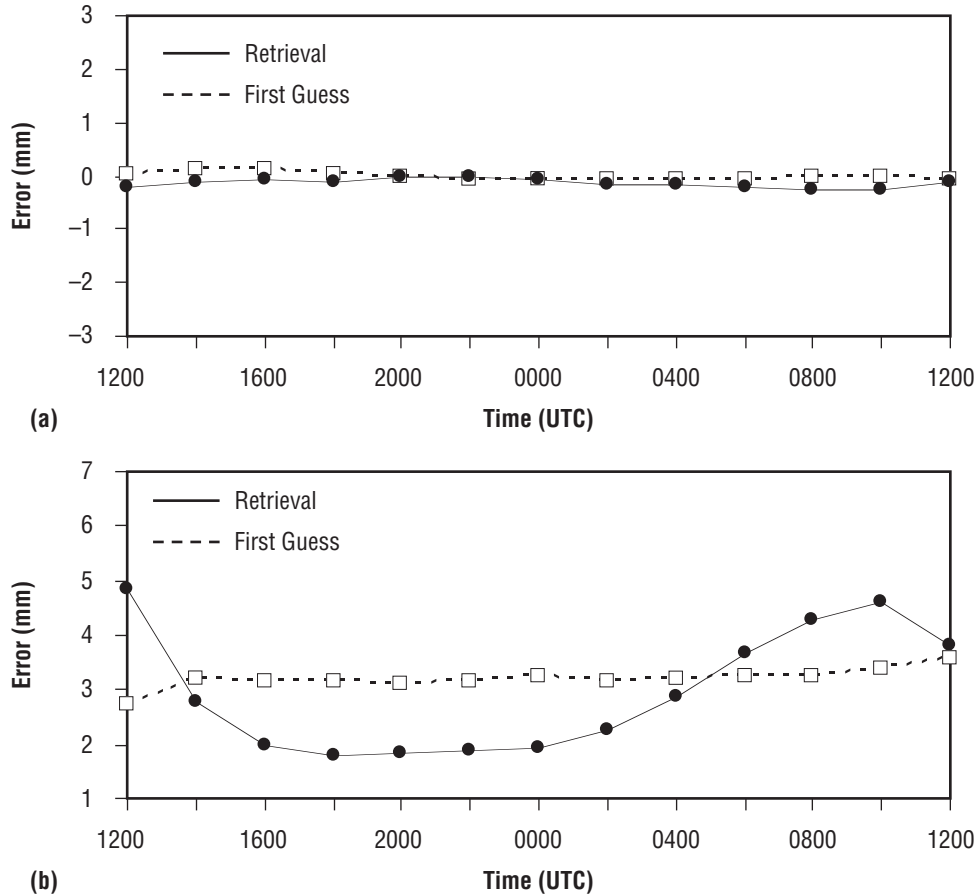


Figure 15. GOES-8 TPW retrieval error statistics as a function of retrieval time for June 17–18, 1986. For this case, the time of the first-guess field is the same as the retrieval time: (a) Mean error (bias) and (b) SD. Dashed line is the error of the first-guess TPW field, and the solid line is the error of the TPW retrieval.

Statistics for the TSKN retrievals from Suggs et al. are shown in figure 16.²⁵ Unlike the TPW retrievals, there is no significant diurnal variation in the retrieval performance. It is seen that the TSKN retrieval bias error is <0.1 K, and the TSKN retrieval SD error is <0.5 K. Note the large first-guess TSKN error is a result of using the surface air temperature. Also, note the lack of sensitivity of the TSKN retrieval SD error to the large first-guess SD error. From this case study it was concluded that TSKN retrieval products, as opposed to TPW products, obtained from actual GOES measurements will have sufficient accuracy and, thus, provide the greatest utility in applications. In order to assess the accuracy of GOESRET TSKN retrievals obtained from actual GOES measurements, other case studies were performed that compared TSKN retrievals from the GOESRET algorithm with TSKN retrieval datasets from other algorithms and ground-based measurements. Example results from these studies are presented in the following paragraphs of this section.

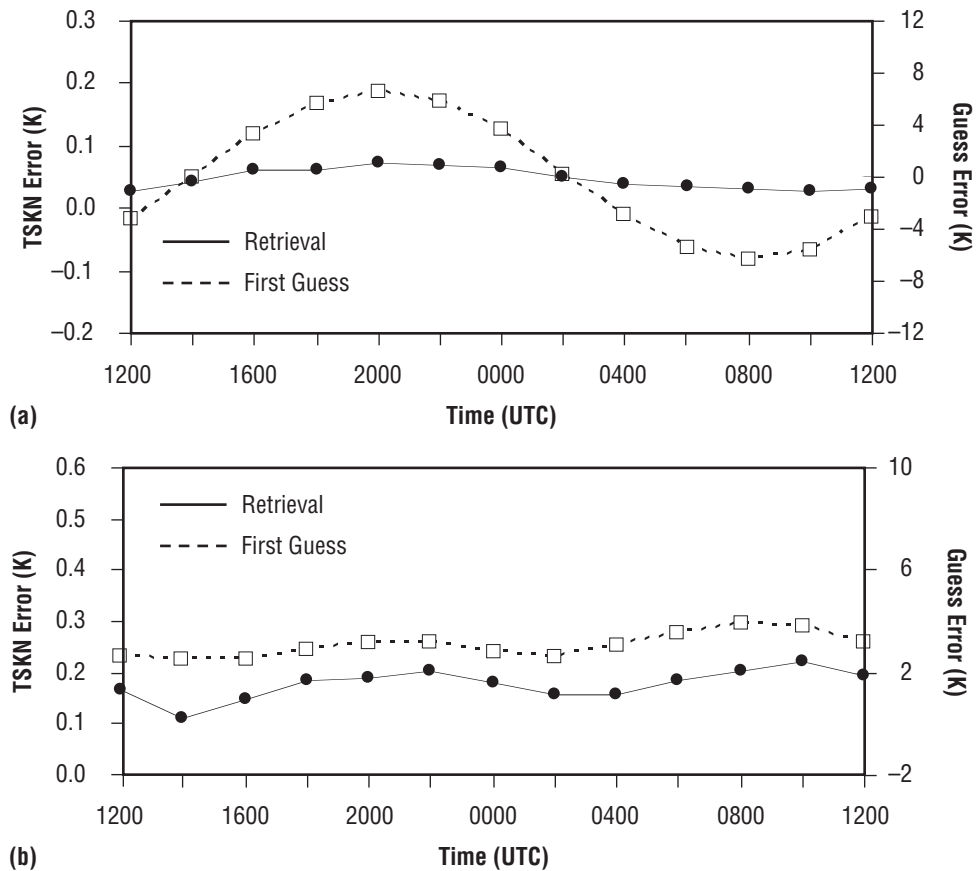


Figure 16. GOES-8 TSKN retrieval error statistics as a function of retrieval time for June 17–18, 1986. For this case, the time of the first-guess field is the same as the retrieval time: (a) Mean error (bias) and (b) SD. Dashed line is the error of the first-guess TSKN, and the solid line is the error in the TSKN retrieval. Guess errors are read from the right axis.

GPGS operational TSKN retrievals from the GOESRET algorithm have been compared to National Environmental Satellite, Data and Information Service (NESDIS) TSKN products. GOES-8 Imager and Sounder retrievals from a September 19, 2000, case study for a domain over the eastern half of the United States are provided as an example. Since the Imager and Sounder have different spatial resolutions (4 and 10 km, respectively) and in order to facilitate a comparison between the two instruments, the Imager and Sounder TSKN retrievals were gridded to a 36-km Lambert conformal grid by applying the appropriate pixel spacing and averaging. Figure 17 shows comparisons of TSKN retrievals from the GOESRET algorithm labeled as GHCC, with retrievals from the NESDIS algorithms for the GOES-8 Imager and Sounder. The comparison shows significant biases between the algorithms for each sensor. The GHCC Imager TSKN (fig. 17(a)) is seen to be cooler than the NESDIS values by 0–2 K, while the GHCC Sounder TSKN is seen to be warmer than the NESDIS retrievals by 1–3 K. The SD errors are between 1 and 2 K. These retrievals include error sources associated with instrument noise calibration biases as well as retrieval methodology differences, such as scene pixel averaging due to the instrument resolution differences. Deficiencies in forward radiation codes are also present. In this case, the GHCC Imager and Sounder retrievals are from the same algorithm while the NESDIS retrievals are from different algorithms.

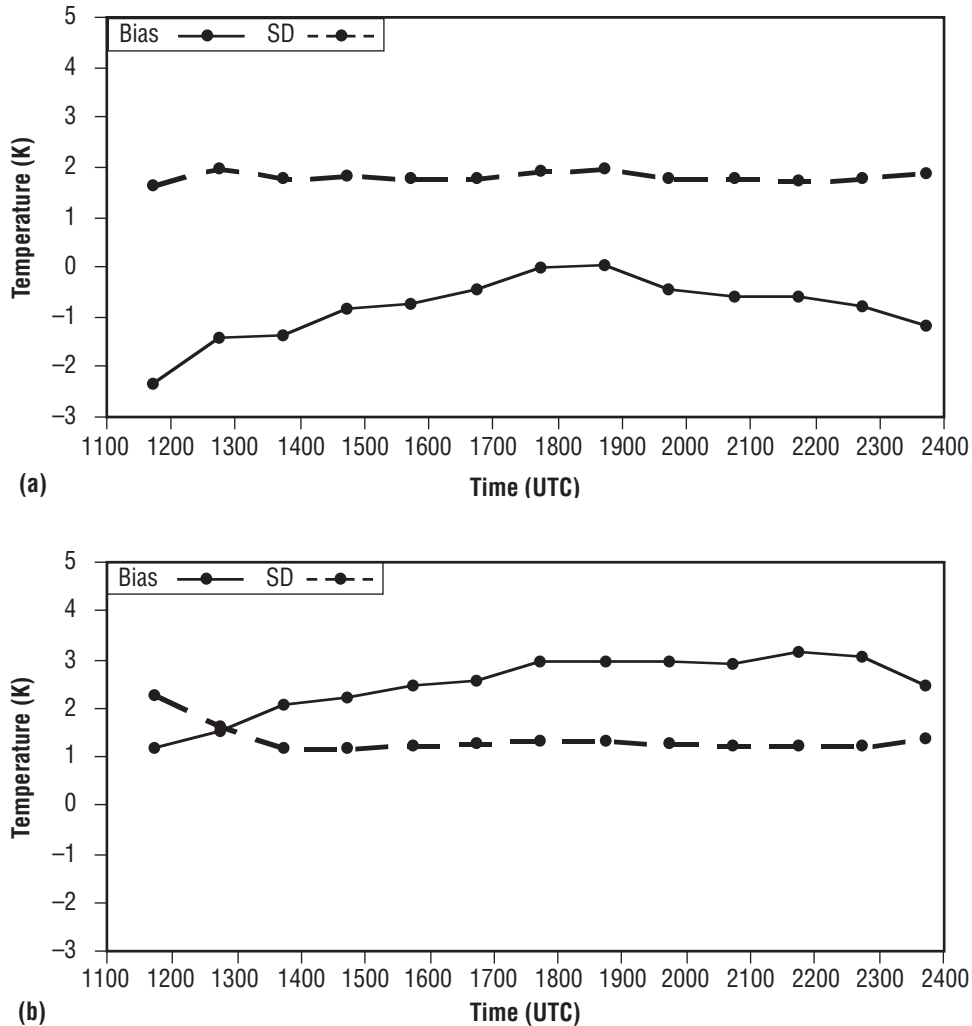


Figure 17. Intercomparison of TSKN retrievals from the GHCC algorithm and the NESDIS algorithm over the eastern half of CONUS on September 19, 2000: (a) Statistical differences between algorithm retrievals when applied to GOES-8 Imager and (b) statistics when algorithms are applied to GOES-8 Sounder.

Figure 18 shows comparisons of TSKN between Imager and Sounder retrievals for GHCC and NESDIS, and suggests that there may be biases between the NESDIS Imager and Sounder algorithms. The NESDIS retrievals (fig. 18(a)) show a large bias on the order of 2–4 K between the TSKN retrievals from the two instruments. In the GHCC comparison (fig. 18(b)), a bias of <1 K is seen. The application of the GOESRET algorithm to both the Imager and Sounder shows fairly consistent results. It is believed that the differences in the GHCC Imager and Sounder retrievals are not algorithm related, but due to instrument noise, calibration, and instrument spatial resolution differences. No conclusion can be drawn on the accuracy of the GHCC retrievals from these comparisons except that the GHCC retrievals lie between those of the NESDIS Sounder and Imager retrievals and, thus, are in general agreement with the NESDIS operational products.

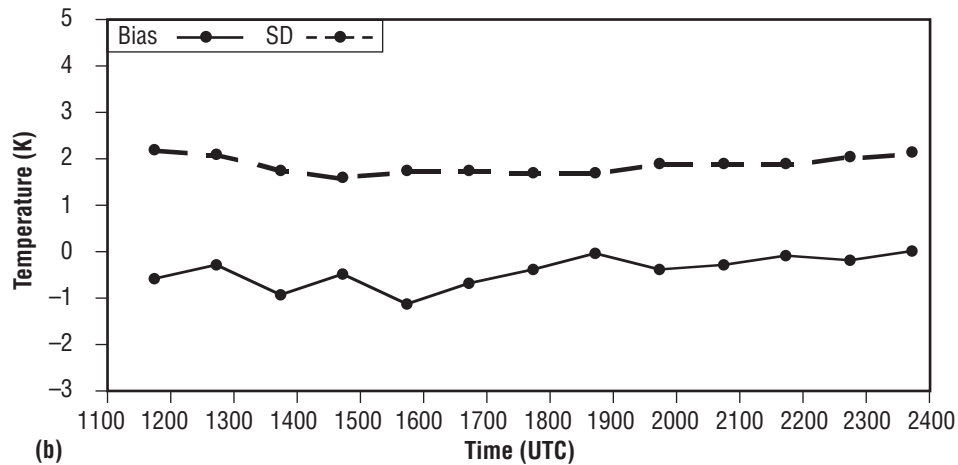
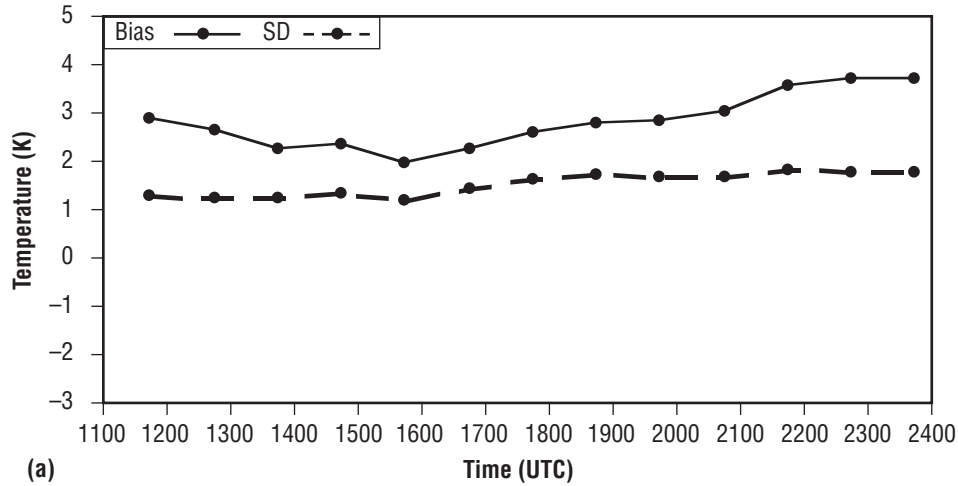


Figure 18. Intercomparison of TSKN retrievals from the GHCC algorithm and the NESDIS algorithm over the eastern half of CONUS on September 19, 2000: (a) Statistical differences between retrievals from NESDIS algorithm applied to GOES-8 Imager and Sounder and (b) statistics when the GHCC algorithm is applied to GOES-8 Imager and Sounder.

Comparisons of TSKN retrievals to ground-based measurements have also been made.²⁶ The ground-based measurements were obtained from the infrared thermometer (IRT), at the Atmospheric Radiation Measurement (ARM) Southern Great Plains central facility site in northern Oklahoma. IRT is a downward-pointing radiation pyrometer mounted on a 25-m tower. IRT provides measurements of the equivalent black body temperature of the scene in its field of view (FOV). An emissivity of 1 is assumed for the scene, which is a wheat field, characteristic of the northern Oklahoma region. Two TSKN retrieval datasets were compared to the IRT measurements. One retrieval dataset was produced by the GOESRET algorithm using GOES-8 Imager data. The other retrieval dataset was produced by NESDIS from the GOES-8 Sounder.

In general, TSKN retrievals are subject to many error sources, such as the instrument noise and calibration stated above, but also, incorrect surface emissivity assignment and cloud or aerosol contamination can be a factor. In this comparison, these effects are present in addition to the effects of comparing datasets with different footprint sizes and discrepancies in the time of retrieval. Figure 18 shows an example of the TSKN from each data source for 2 days of the study period. For both days shown, the TSKN values from GOES-8 show good agreement with each other and are within 1.5 K of the IRT TSKN values in the early morning hours. However, after the early morning hours, the GOES-8 TSKN values begin to diverge from the IRT values, showing the maximum difference at the peak heating of the day, ≈ 2000 UTC. This trend of an increasing bias as peak heating approaches is consistent for all the study days, but the magnitude of the bias between days is variable, as seen in figure 19. Possible causes for the midday temperature biases may be due to the large area footprint associated with the GOES-8 TSKN as compared with the relative point source measurement of the ARM IRT instrument. Also, difference in the sensor FOV slant-path angle of the satellite and ground-based IRT may be a factor. The FOV slant path from GOES-8 to the ARM Southern Great Plains location is $\approx 48^\circ$ with respect to zenith.

Of main interest in the TSKN comparison is the agreement in the early morning time rate of change of TSKN or tendency since this quantity provides information about moisture availability and can be assimilated into numerical models. Even though error biases may exist in the TSKN retrieval due to the error sources stated previously, it is anticipated that the early morning TSKN tendency will be preserved in the retrievals. The early morning TSKN 1-hr tendencies were calculated for the clear-sky days during the study period. These values are presented in figure 20. The days with missing data are primarily attributed to cloudy days over the ARM Southern Great Plains site—except for August 26, when there were no morning IRT measurements. Also, some days show only one GOES-8 source due to the unavailability of that particular hour's retrieval due to various data acquisition problems.

It is seen in figure 20 that the TSKN tendencies vary from day to day and even between hours. In general, the GOES-8 derived TSKN tendencies agree fairly well with the ground-based IRT measured tendencies and capture the variability and trend seen in the IRT measurements. The differences between the GOES-8 and the IRT tendencies calculated with respect to the IRT values are given in table 3. The mean relative differences between the GOES-8 and IRT tendencies are <15 percent, except for the GOES-8 Sounder 1345–1245 UTC value, which could be an artifact of the low number of sample days. The results of this study suggested that the GOESRET algorithm could provide retrieved GOES-8 Imager TSKN morning tendencies at a sufficient accuracy for model assimilation.

Results from case studies involving the assimilation of TSKN tendencies into the PSU/NCAR MM5 to improve model forecasts have been promising. One particular case study is presented here to not only demonstrate the improvement in model forecasts by the assimilation of TSKN tendencies but also to show the effects on the forecasts due to GOES instrument noise and spatial resolution differences.²⁷ It was found that by applying the appropriate retrieval methodology to create datasets with resolutions that are consistent with the model grid resolution and, at the same time, minimizing the effects of measurement noise, model assimilation results are improved. Figure 21 shows TSKN retrieved tendencies over the Southeast on a 12-km Lambert conformal grid from the GOES-8 Imager and Sounder using three different retrieval spatial averaging scenarios. For the Imager product (fig. 21(a)), 3- by 5-pixel averaging was performed during the retrieval process to provide a footprint consistent with a grid box of 12 km. Two Sounder products were created: (1) A single-pixel retrieval (fig. 21(b)) and (2) a 3- by 3-pixel averaged retrieval (fig. 21(c)). The single-pixel Sounder retrieval provides a smaller, higher resolution footprint but without the advantage of pixel averaging

to reduce measurement noise. The 3- by 3-pixel Sounder retrieval provides a larger footprint (on the order of 30 km) but uses pixel averaging to reduce the noise. Figure 21 illustrates that differences exist between the three products. The Sounder single-pixel product appears to have more structure than the other two, and thus, it can be argued that the Sounder single-pixel product may provide more information to the model in the assimilation process.

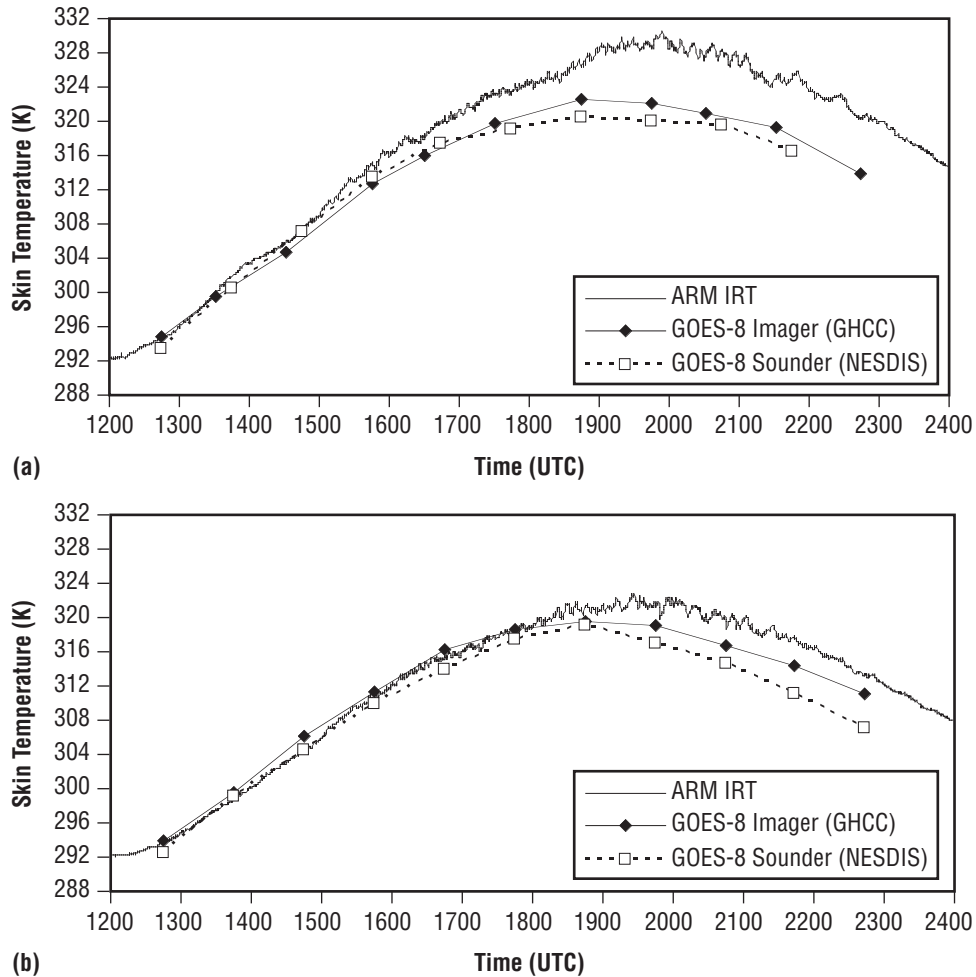


Figure 19. Comparison of TSKNs measured at the ARM Southern Great Plains site by the ground-based IRT instrument with TSKNs retrieved from GOES-8 Imager and Sounder infrared channel measurements: (a) August 18, 1999, and (b) September 1, 1999. The Imager retrievals were obtained from the GHCC algorithm while the Sounder retrievals were obtained by NESDIS.

A methodology for assimilating the tendency of GOES-8 TSKN retrievals into a mesoscale model has been implemented at GHCC.¹ The assimilation technique is based on results from numerous studies showing that TSKN tendencies during the midmorning hours are very sensitive to the surface moisture availability—an integrated function of surface characteristics, such as soil wetness and vegetation—and less sensitive to other parameters, such as surface roughness.

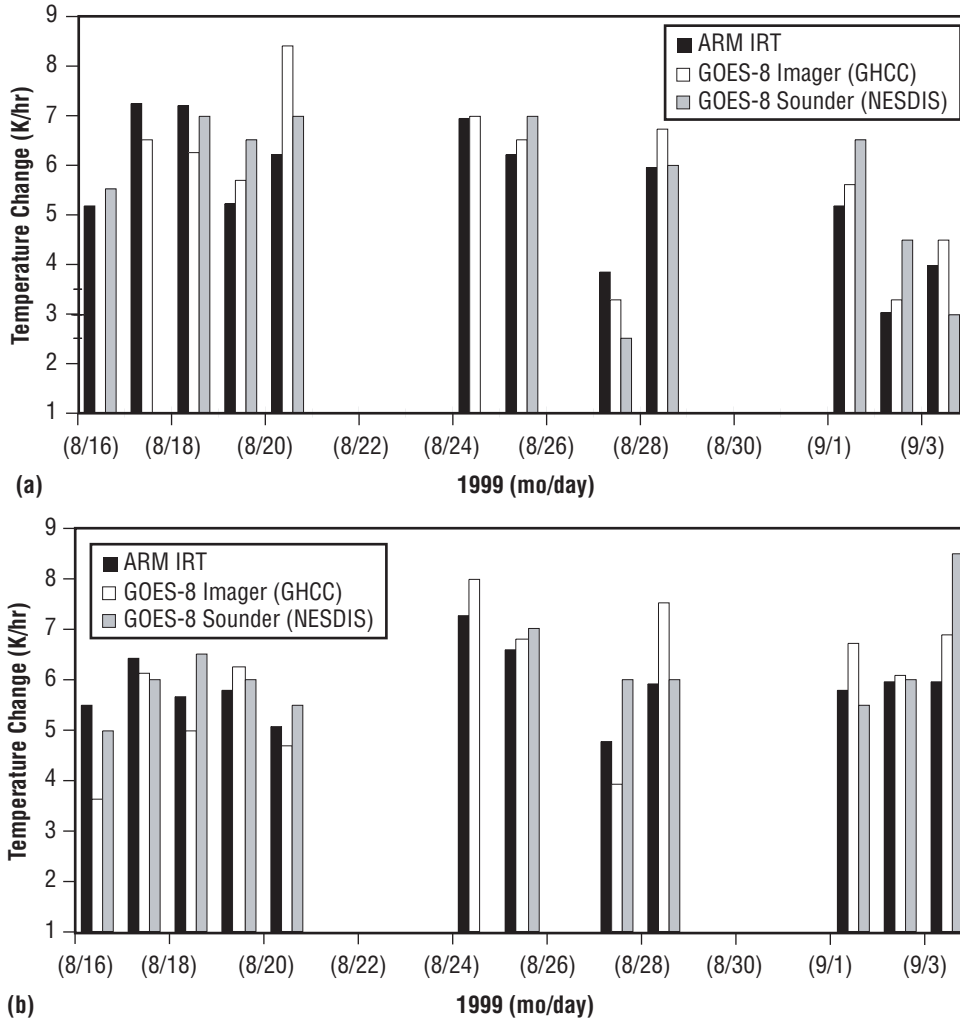


Figure 20. Comparison of early morning TSKN tendencies measured at the ARM Southern Great Plains site by the ground-based IRT with TSKNs retrieved from GOES-8 Imager and Sounder infrared channel measurements: (a) From 1345 to 1245 UTC and (b) from 1445 to 1345 UTC. The Imager retrievals were obtained from the GHCC algorithm while the Sounder retrievals were obtained by NESDIS.

Table 3. Mean absolute relative differences between GOES-8 retrieved TSKN tendencies and IRT measured tendencies.

| GOES-8 Instrument (Algorithm) | Tendency Difference | |
|----------------------------------|---------------------|---------------|
| | 1345–1245 UTC | 1445–1345 UTC |
| Imager (GHCC) | 12(%) | 13(%) |
| Sounder (NESDIS) | 19(%) | 11(%) |

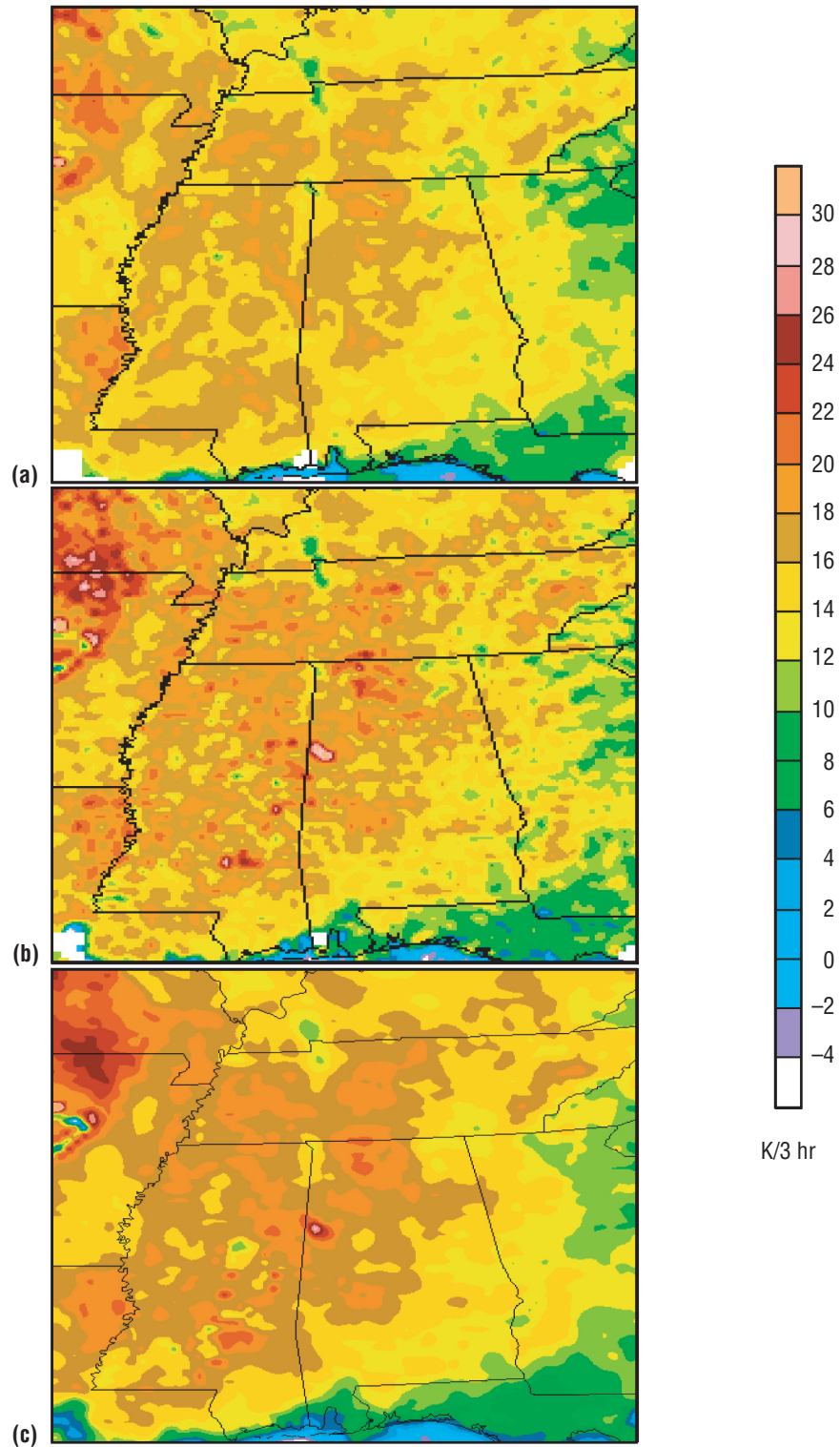


Figure 21. TSKN 3-hr tendencies (1245–1545 UTC) September 19, 2000. Tendencies are applied to a 12-km Lambert conformal grid using GOES-8 (a) Imager retrievals (≈ 4 -km resolution) with 3- by 5-pixel smoothing, (b) Sounder retrievals (≈ 10 -km resolution) single-pixel per grid assignment, and (c) Sounder retrievals (≈ 10 -km resolution) with 3- by 3-pixel smoothing.

Based on these results, McNider et al. developed a simple strategy to dynamically assimilate GOES TSKN tendencies into the surface energy budget of a mesoscale model.²⁸ Lapenta et al. has applied this technique within the latest release of the PSU/NCAR MM5.¹

For this case study, a total of four 12-hr forecasts from the 1200 UTC cycle of September 19, 2000, were performed. Initial conditions were produced from the National Centers for Environmental Prediction (NCEP) Eta Data Assimilation System (EDAS) analysis on the 40-km Advanced Weather Interactive Processing System (AWIPS) grid and lateral boundary conditions extracted from the early Eta forecast. A nested grid configuration was used with a 36-km CONUS and a 12-km nest over the Southeast and assimilation runs were made using each of the TSKN tendency products described previously (fig. 21). Tendencies were calculated from hourly retrievals and assimilated between 1245 and 1545 UTC. A fourth forecast was made as a control run with no data assimilation and used the simple Blackadar force-restore slab model to represent land-surface forcing. The impact of assimilating the TSKN tendencies on the model forecast was determined via verification statistics of the 9-m air temperature. An indication of the significance of the Sounder and Imager TSKN differences discussed above is reflected in the model forecast differences.

The results of verification statistics from three model forecasts are presented in figure 22. The statistics represent the near-surface air temperature bias and RMSE based on ≈ 80 hourly observations for each hour of the 12-hr forecast. The statistics are presented as the relative improvement in the model forecast with respect to the control run. The statistics indicate that the assimilated TSKN tendencies improve the model forecast of surface air temperature in each case. The least improvement comes from the Sounder single-pixel retrievals. Even though these retrieval tendencies appear to exhibit more spatial structure (fig. 21(b)), this structure is probably an artifact of the measurement noise. The model's best performance is provided by the Imager tendencies. The higher resolution Imager FOV allows a greater number of pixels to be averaged and, at the same time, be consistent with the model grid size.

The case studies above demonstrate that the GOESRET algorithm can provide quality TSKN retrieval data products with sufficient accuracy to be used in data assimilation studies and other applications. Work is in progress to assess the quality of daytime TPW retrievals and improve the algorithms' performance for nighttime TPW retrievals.

3.3.6 ASCII File Generation Module

The purpose of the ASCII file generation module is to integrate and grid the output of the previous modules to produce a dataset in a single ASCII file. For example, the TSKN, TPW, CTP, visible-channel data, and MASK information are combined into a single file on a grid defined by the user. Spatial averaging of the retrieval values is performed when necessary to be consistent with the grid resolution. Clear-sky and cloudy grids are designated from the input MASK. A clear-sky grid is one where the percent number of clear pixels being averaged exceeds an input threshold value. The output file is a data product typically provided to users requiring the GPGS retrievals on a specific grid and resolution, often consistent with a numerical model grid.

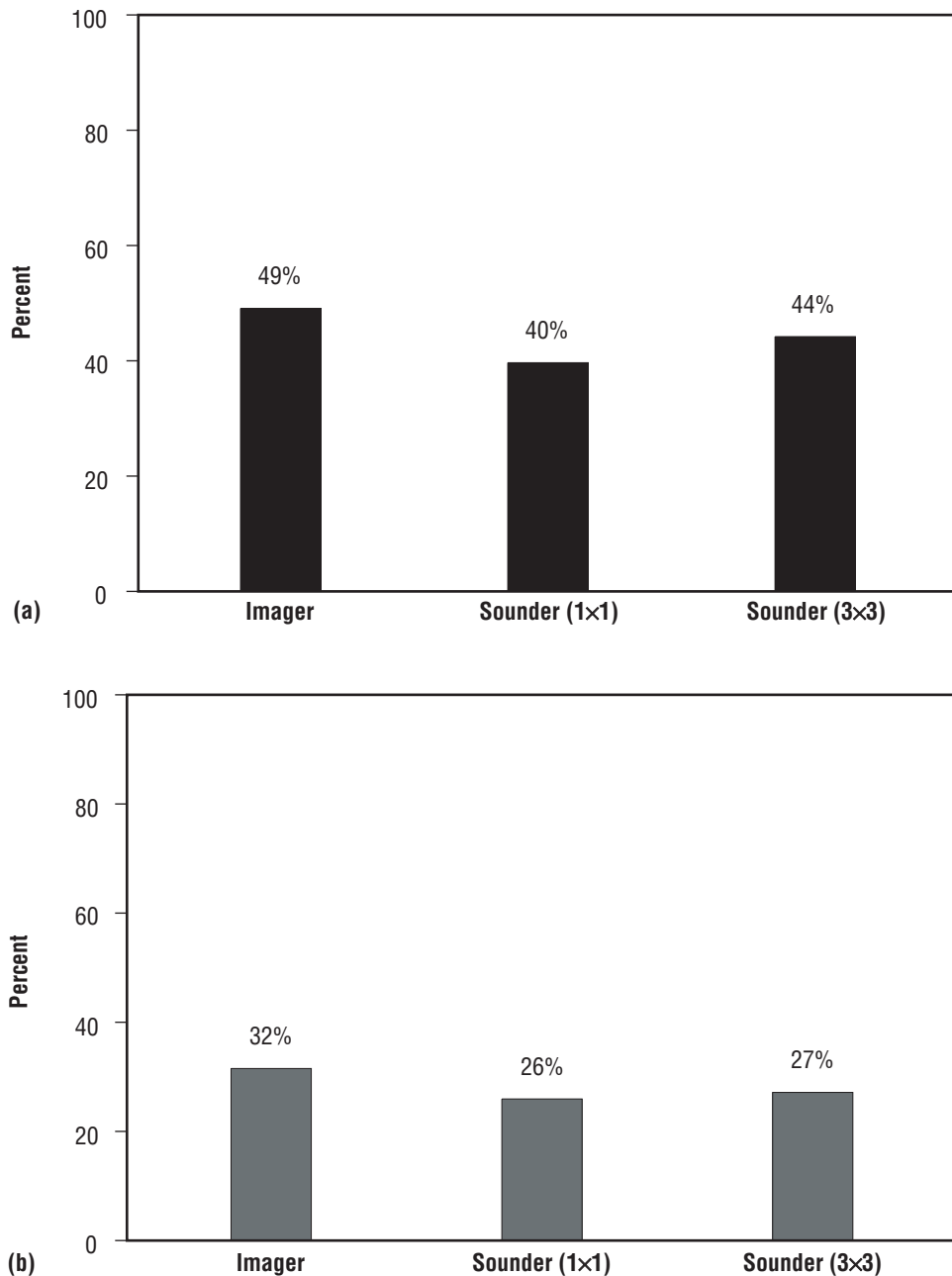


Figure 22. MM5 9-m surface air verification statistics using different assimilated GOES-8 retrieval TSKN products. All data is at 12-km grid resolution but obtained from different instrument pixel resolutions and number of pixels smoothed (fig. 21): (a) Bias improvement and (b) RMS improvement. Verification statistics relative to MM5 control run.

The inputs to the module are the McIDAS areas—MASK, CTP, ALB, CLDALB, INS, TSKN, and TPW—from the previous modules of the processing unit of GPGS. The visible-channel area can also be input. The input of any of these files is optional. In addition to the retrievals, a location file of

latitudes and longitudes that define the grid is a required input. A second input option exists for input of the TSKN and TPW data. If the output from GOESRET was an ASCII file of TSKN and TPW retrievals; i.e., grid data not at pixel resolution, then this ASCII file is the input into the ASCII file generation module. In this case, the retrieval locations are taken from this file (input of location file not required) and all retrieval parameters are gridded to be consistent with the TSKN and TPW values in the output GOESRET ASCII file. Also, when the GOESRET ASCII file is used as an input, TSKN and TPW quality flags are passed along to the gridded output file. In addition to the input files, command line input control parameters exist to control the amount of pixel averaging and the percent of cloudy pixels that define a clear or partly cloudy grid.

The output of this routine is an ASCII file that contains the retrieval values of TSKN, TPW, ALB, INS, CLDALB, and CTP if the corresponding parameter input files are provided. Similarly, visible-channel planetary ALB is also present if its input file is provided. The file also contains the latitudinal and longitudinal coordinates of the grid locations and a cloud flag. When the GOESRET ASCII file is input, the output file will also contain brightness temperature values from one of the infrared channels used in the retrieval of TSKN and TPW along with GOESRET algorithm flags. A detailed description of the data file is provided in appendix A.

3.4 Postprocessing

The postprocessing unit of GPGS is responsible for generating images of the retrieved products for archiving and quality control purposes and to display on the Web. The images can be in the original GOES projection at pixel resolution, or of gridded retrievals in projections, domains, and resolutions defined by particular forecast models. For example, for the Texas 2000 Air Quality Study there were three domains that the products were generated on, each a Lambert conformal projection with resolutions (36, 12, and 4 km) that became progressively higher as the domain size decreased.⁴

To generate the gif images, 1-byte areas of the products are displayed, color enhanced, and the resulting image saved, all within McIDAS. The output from the retrieval process is either in the format of 2-byte areas or ASCII files, and therefore, the postprocessing unit involves generating the 1-byte areas that can be displayed in McIDAS. If the input is the reformatted ASCII file, then there is a utility program that accepts the ASCII file, a template area—remapped into the required projection and resolution if necessary—and the product name as inputs. The utility program reads the selected product from the ASCII file and writes the values into a new area with the same projection as the template area, and the output being a 2-byte area. To generate a 1-byte area, a McIDAS command is used to scale the product values to within a 0–255 range, producing an area for which the calibration of the product values is now known by McIDAS, and the user and the area can be displayed with a custom designed color enhancement and bar.

Once a 1-byte area has been generated, displayed, and color enhanced, the result is saved, currently in gif format within McIDAS. The gif image may then be cropped and a smaller thumbnail image generated using the ImageMagick™ convert command. In real-time mode, the cropped and thumbnail images are then sent to the GHCC Web server, <http://www.ghcc.msfc.nasa.gov/goesprod/>, via FTP, where the past 2 week's images are maintained. Figure 23 shows some examples of how the products are displayed on the Web page. In case-study mode, a Web page for the case study is generated, and

images of each of the products in all of the domains are available on the Web site. On both the real-time and case-study Web pages, animated, interactive movie loops of the products are available. The original gif images are archived for possible future reference.

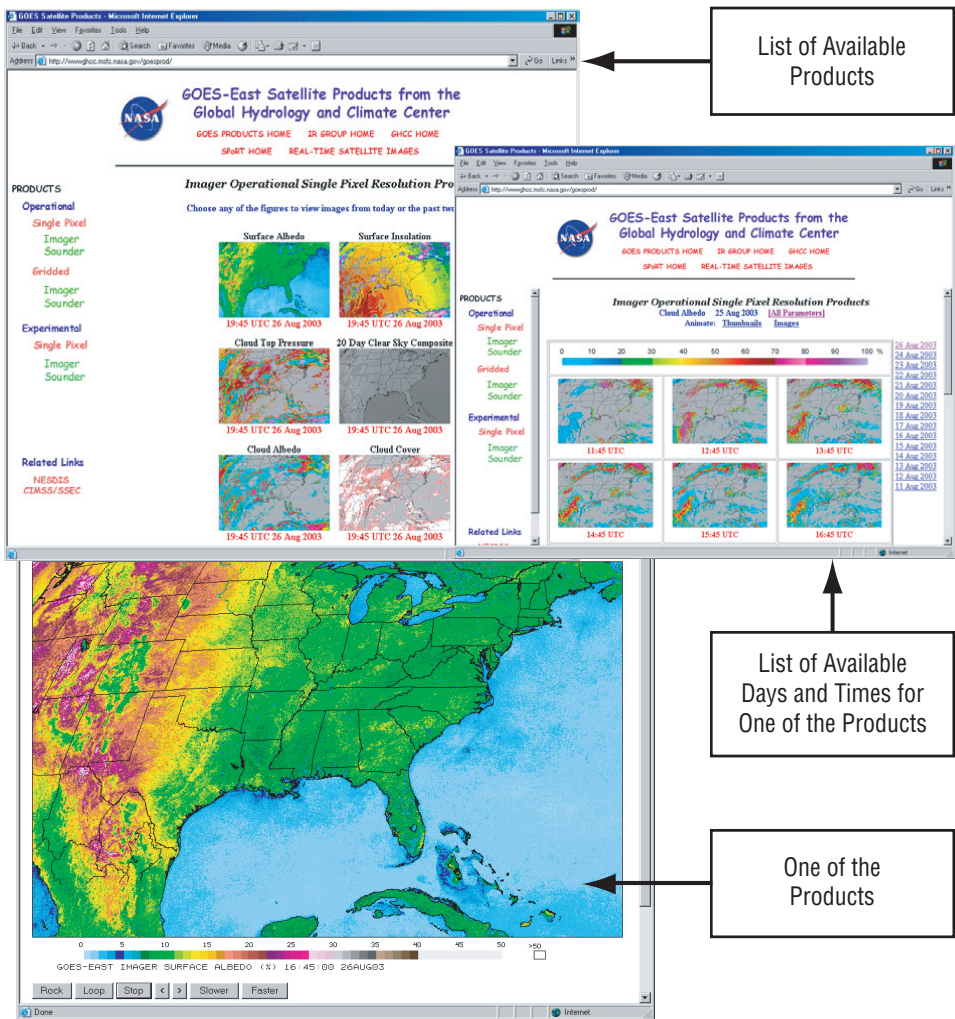


Figure 23. Examples of Web page displays of the real-time GOES products.

In case-study mode, postprocessing can also involve sending the ASCII files of the retrievals to the Web page, providing documentation of the products, domain coverage, etc. for the particular case on the Web, and also generating CDs of the data, images, and documentation.

A final step in postprocessing is archiving all of the products and images generated in the three steps of GPGS. At GHCC, a large, long-term archive system that allows the retention all of the GOES data and retrievals is available for possible future use. In real-time mode, a script runs once a day that moves all the files created during a single day’s retrievals process to the long-term archive system and then deletes those files from the local system. This archiving process allows GPGS to run on a Unix or Linux machine, unattended and without the worry of disk space being filled.

4. GOES PRODUCT GENERATION SYSTEM FUTURE IMPROVEMENTS

The GPGS software and scripts are regularly modified to improve their performance. Over the last few years, significant improvements in the geophysical parameter retrieval methodology have been made and incorporated into the GPGS procedures. Additional changes are planned for the future. A number of the planned improvements focus on the guess—the retrieval algorithms require a priori or guess information to help constrain the solution—while others incorporate additional ancillary data or deal with specific changes to the retrieval algorithms. The algorithm and procedural changes under consideration are described in section 4.1.

4.1 Radiative Transfer Algorithms

Probably the most needed improvement to the GPGS code concerns the transmittance calculations required to produce guess radiances in the various GOES channels. The current approach for transmittance calculations is based on a narrow band regression approach developed over 30 yr ago and has not been modified extensively since that time.⁸ The code that implements this scheme at GHCC is affectionately known as SIMRAD. SIMRAD also uses the calculated transmittances in the radiative transfer equation to calculate spectral radiances that are convoluted with channel response functions to obtain channel radiance or brightness temperature values. Garand et al. have shown that SIMRAD produces significant biases in the infrared window region when compared to modern line-by-line formulations.²⁹ In the Garand et al. study, television infrared observation satellite operational verticle sounder high-resolution infrared sounder (HIRS) channel-10 (12.5 μm) brightness temperatures were simulated for an ensemble of 42 diverse profiles representing a variety of thermal and moisture conditions around the globe. A mean cold bias of -1.18 K with an SD of 1.03 K was noted. These errors are much larger than most other transmittance or radiative transfer models. While these results were for the HIRS 12.5- μm channel, the results are directly transferable to the GOES Imager and Sounder split-window channels where similar water-vapor absorption processes occur. Errors of this magnitude in the guess brightness temperatures will significantly contribute to the errors in the retrieved TSKN and TPW fields.

The calculation of the first-guess transmittances and subsequent guess channel radiances use a profile of temperature and moisture from the top of the atmosphere down to the station pressure. The station pressure is available as part of the guess information. For pressures $<1,000$ mb, interpolation is used between radiative transfer model levels. No interpolation or extrapolation is performed for pressures $>1,000$ mb, the lowest radiative transfer model level. Future changes in either the SIMRAD formulation or the new radiative transfer model algorithm will incorporate calculations down to the station pressure for all guess locations. Additionally, in some instances, the station pressure provided in the guess data is not representative of the large terrain height changes over mountainous regions. Planned changes to the radiative transfer code will include a correction to the guess-data station pressure in these mountainous regions.

4.2 Cloud Retrieval Physics

While the MASK information is important for the determination of clear regions for atmospheric and surface parameter retrievals, CTP or height information is a value added product. Currently, the CTP is inferred from an infrared look-up method with a reference temperature profile. For opaque clouds, this method yields a CTP accurate to within about 25 to 50 mb. However, for nonopaque clouds such as thin cirrus, this method can produce large overestimates of the CTP. The carbon dioxide (CO₂) slicing method uses additional channels in the CO₂ absorption band to account for the varying opacity of these clouds and produces a less biased pressure estimate.^{30,31} This approach can be applied to the GOES Sounder data, which include several CO₂ channels in the 13- μ m region and GOES-12 Imager, which includes one channel at 13.3 μ m.

4.3 Use of Ancillary Data

An underlying assumption in the retrieval of TSKN and TPW is that the surface thermal emissivity in the 11- and 12- μ m channels is known, and assumed to be constant in space and time. In reality this is not the case and the real value of emissivity cannot be easily measured from the ground for the satellite footprint. Estimates of the surface emissivity at several infrared wavelengths are now routinely available from the moderate-resolution imaging spectroradiometer (MODIS). Suggs et al. have shown that information obtained from the MODIS-derived surface emissivities may be able to improve the retrieval of TSKN from GOES.³² Incorporating this information into operational GOES retrievals at GHCC should improve the quality of both the TSKN and TPW values.

4.4 Guess Information

A priori information is used in many of the retrieval algorithms to provide background training or guess information. Suggs et al. have shown that the accuracy of the derived TSKN and TPW products is dependent on the quality of the first-guess information.²⁵ For the retrieval of the atmospheric parameters, TSKN, TPW, and CTP, the regional MM5 output at 36- or 12-km grid resolution, run twice daily at GHCC, provides predicted temperature and moisture information as a function of pressure. While this guess information is convenient—available hourly at retrieval times—and reasonably accurate, it does not provide the flexibility to easily extend the algorithm to other regions because of the limited extent of the MM5 domain. It also does not provide commonality with other operational retrieval products; e.g., NESDIS, that use operational forecast model guess information. The adaptation of the guess preparation modules used in GPGS for the Eta or other operational model data, which cover a larger domain, is being planned.

The algorithms for the retrieval of INS and ALB products currently use fixed water vapor information—a single value of TPW—in its calculations of the attenuation of solar radiation through the atmosphere. The use of spatially and temporally varying TPW information from the numerical model guess data (described above) will substantially improve the theoretical and physical accuracy of the attenuation calculations as well as the subsequent derived products.

4.5 Portability of Code

The processing of satellite data for the retrieval of geophysical parameters and subsequent use in an operational research setting often requires accurate calibration and geolocation of the imagery accounting for satellite view angle and Earth curvature effects. The satellite data used in GPGS is preprocessed using McIDAS software modules. The use of McIDAS in GPGS has several major advantages, as follows:

- McIDAS has been used to calibrate, navigate, and display weather satellite data at NASA's Marshall Space Flight Center since 1981. Numerous unique processing algorithms and functions have been developed in McIDAS for these applications.
- The real-time GOES data collected with the NASA/The University of Alabama in Huntsville satellite ground stations at GHCC is disseminated (to Web and FTP servers) using McIDAS code to remap the data into specific projections and archived in unique McIDAS data formats. This makes access and redisplay quick and easy.
- Significant expertise in McIDAS programming and applications has been acquired over the years and maintained at GHCC.

All of these factors have contributed to the development of the McIDAS-based GPGS system without the use of significant levels of manpower that are often required to develop and maintain an operational system for processing satellite data. New applications of the products of the GPGS system and use by other satellite ground-station operators are precluded by this proprietary code. A non-McIDAS version of GPGS is being considered to address such users and applications.

APPENDIX A—ASCII DATA FILE DESCRIPTION

When retrievals generated by GPGS are required on a specific grid, the final output is in ASCII file format. This ASCII file contains the retrieval values of TSKN, TPW, ALB, INS, CLDALB, and CTP if the corresponding parameter input files are provided. Similarly, visible-channel planetary ALB is also present if its input file is provided. The file also contains the latitudinal and longitudinal coordinates of the grid locations as well a cloud flag. When the GOESRET ASCII file is input to the ASCII file generation module, the output file will also contain brightness temperature values from one of the infrared channels used in the retrieval of TSKN and TPW along with GOESRET algorithm flags. Figure 24 shows an example of one of the ASCII files.

There are three lines of header information. Line 1 contains the date, time, and a short memo. Line 2 indicates the version number of the code used to generate the ASCII file (version 3+), the satellite sensor (GOES-8 Imager), the grid description (Lambert conformal with center longitude of 100°, and true latitudes of 30° and 60°, and resolution of 12 km), the box size of pixels averaged for each grid location (3×5), and the percent of pixels in the box required to be clear/good for a retrieval to be produced (66 percent). Line 3 provides the column header information—table 1 provides a description of the parameters in the file.

Missing values, such as locations in space, are given by -999.0 (-999 for integer parameters). A quality flag is provided for each pixel that is generated from the TSKN/TPW retrieval algorithm. These quality flags are intended for internal use to monitor the retrieval algorithm's performance and should not normally be considered by the end user. In general, a valid retrieval has a quality flag value of 0 or -1,000. Retrieval values are also provided when the data values are out of bounds, but these data should be considered suspect. A retrieval may meet more than one quality condition, and in that case, the flag value is the sum of the individual flag values. For example, a retrieval where the observed and guess brightness temperature difference condition is not met and the TPW retrieval is out of bounds has a quality flag value of $-1,000 + -90 = -1,090$. Table 4 provides a list of the parameters that are provided in the ASCII files and the valid range and comments for each parameter.


```

20000825 2000238 184500 DATE(cal), DATE(julian), TIME(UTC) MEMO: Tex2000
VRS: 3 SEN: G8I GRID: LC_100_30_60_12 BOX: 3 5 PCTPIX: 66
RET LAT LON SATVIS(%) SATIR(K) CLDFLG TFW(mm) TSKN(K) SFCALB(%) INSL(W/m2) CLRSKY(%) CTP(mb) CLDALB(%) QFLAG
1 25.994 100.654 12.3 310.2 1 0.0 0.0 17.9 1000.8 0 916 9.9 -1000010
2 26.000 100.533 13.5 307.6 1 0.0 0.0 14.6 963.4 0 908 12.8 -1000010
3 25.996 100.409 7.5 301.3 1 0.0 0.0 10.1 998.3 0 892 10.4 -1000010
4 26.003 100.289 11.6 306.4 1 0.0 0.0 13.0 985.3 0 917 10.6 -1000010
.....
178 25.693 91.482 4.2 291.7 0 70.0 309.8 2.2 1010.0 87 807 0.0 -90
179 25.680 91.368 4.3 290.6 1 0.0 0.0 2.4 1009.9 60 826 0.0 -10
180 25.667 91.249 4.6 291.0 0 70.0 308.1 2.3 1004.8 87 807 0.0 -1090
181 25.664 91.131 5.2 292.1 0 70.0 308.6 2.4 977.1 73 833 21.7 -90
182 25.651 91.017 4.6 293.7 0 64.2 308.1 2.2 985.6 93 896 29.3 0
.....
7350 33.953 97.694 9.3 311.6 0 42.8 327.0 14.5 969.0 87 984 5.1 -9001000
7351 33.948 97.562 9.4 310.7 0 43.0 326.7 14.2 968.7 87 984 5.5 -1000
7352 33.942 97.424 8.6 309.7 0 42.7 325.3 13.4 972.0 100 0 0.0 -1000

```

Figure 24. An example of an ASCII file generated by GPGS.

Table 4. Description of the parameters provided in the GPGS ASCII files.

| Name | Parameter | Data Range | Comment |
|--------|--|--|---|
| RET | Retrieval No. | 1–No. grid points | Grid point sequence number |
| LAT | Latitude (deg) | Grid dependent | Grid box center latitude |
| LON | Longitude (deg) | Grid dependent | Grid box center longitude (+west) |
| IR | Brightness temperature (K) | | GOES longwave IR brightness temperature |
| VISALB | Planetary albedo (%) | 1–100 | Visible-channel albedo value |
| CLDFLG | Cloud flag No cloud | 0 1 | No cloud Cloud present |
| TPW | Total precipitable water (mm) | 1–70 0 | Clear-sky values Retrieval attempted; no value returned due to clouds, bad data, or algorithm failure |
| TSKN | Skin temperature (K) | 244–327 0 | Clear-sky values Retrieval attempted; no value returned due to clouds, bad data, or algorithm failure |
| SFCALB | Surface albedo (%) | 0.1–100 | 20-day clear-sky composite value |
| INSL | Surface insolation (W/m ²) | 0–1,200 | |
| UPX | Usable No. of pixels (%) | 0–100 | % of noncloudy pixels used in obtaining a gridded retrieval |
| QFLAG | Quality flag | 0 –1 –10 –90 –100 –1,000 –10,000 –100,000 –1,000,000 –9,000,000 | TSKN and TPW retrieval passed checks View angle of guess and observation greater than limit Too many cloudy pixels in grid box TPW retrieval out of bounds Solution matrix inversion condition not met Observed and guess temperature difference condition not met Solution matrix residual condition not met TSKN convergence failed No pixels clear or usable TSKN retrieval out of bounds |

REFERENCES

1. Lapenta, W.M.; Suggs, R.J.; Jedlovec, G.J.; et al.: "Impact of Assimilating GOES-Derived Land Surface Variables Into the PSU/NCAR MM5," Preprint, *Workshop on Land-Surface Modeling and Applications to Mesoscale Models*, Nat. Ctr. Atmos. Res., Boulder, CO, pp. 65–68, 1999.
2. Suggs, R.J.; Jedlovec, G.J.; and Lapenta, W.M.: "Satellite Derived Land Surface Temperatures for Model Assimilation," Preprint, *3d Conference on Integrated Observing Systems*, Amer. Meteor. Soc., Dallas, TX, pp. 205–208, 1999.
3. Jedlovec, G.J.; Haines, S.L.; Suggs, R.J.; et al.: "Use of EOS Data in AWIPS for Weather Forecasting," Preprint, *20th Conference on Weather Analysis and Forecasting and 16th Conference on Numerical Weather Prediction (CD-ROM)*, 2.2. Amer. Meteor. Soc., Seattle, WA, 2004.
4. "Texas Air Quality Study," University of Texas at Austin (online), URL: <http://www.utexas.edu/research/ceer/texaqs> Last accessed February 17, 2004.
5. Hafner, J.; and Kidder, S.Q.: "Urban Heat Island Modeling in Conjunction With Satellite-Derived Surface/Soil Parameters," *J. Appl. Meteor.*, Vol. 38, pp. 448–465, 1999.
6. Menzel, W.P.; and Purdom, J.F.W.: "Introducing GOES-I: The First of a New Generation of Geostationary Operational Environmental Satellites," *Bull. Amer. Meteor. Soc.*, Vol. 75, pp. 757–781, 1994.
7. Lazzara, M.A.; Benson, J.M.; Fox, R.J.; et al.: "The Man Computer Interactive Data Access System: 25 Years of Interactive Processing," *Bull. Amer. Meteor. Soc.*, Vol. 80, pp. 271–284, 1999.
8. McMillin, L.M.; and Fleming, H.E.: "Atmospheric Transmittance of an Absorbing Gas: A Computationally Fast and Accurate Transmittance Model for Absorbing Gases With Constant Mixing Ratios in Inhomogeneous Atmospheres," *Appl. Opt.*, Vol. 15, pp. 358–363, 1976.
9. Guillory, A.R.; Lecue, J.M.; Jedlovec, G.J.; et al.: "Cloud Filtering Using a Bi-Spectral Spatial Coherence Approach," Preprint, *9th Conference on Satellite Meteorology and Oceanography*, Amer. Meteor. Soc., Paris, France, pp. 374–376, 1998.
10. Jedlovec, G.J.; and Laws, K.: "Operational Cloud Detection in GOES Imagery," Preprint, *11th Conference on Satellite Meteorology and Oceanography*, Amer. Meteor. Soc., Madison, WI, pp. 412–415, 2001.
11. Jedlovec, G.J.; and Laws, K.: "GOES Cloud Detection at the Global Hydrology and Climate Center," Preprints, *12th Conference on Satellite Meteorology and Oceanography (CD-ROM)*, P1.21, Amer. Meteor. Soc., Long Beach, CA, 2003.

12. Fritz, S.; and Winston, J.S.: "Synoptic Use of Radiation Measurements From Satellite TIROS-II," *Mon. Weather Rev.*, Vol. 90, pp. 1–9, 1962.
13. Jedlovec, G.J.; Lerner, J.A.; and Atkinson, R.J.: "A Satellite-Derived Upper-Tropospheric Water Vapor Transport Index for Climate Studies," *J. Appl. Meteor.*, Vol 39, pp. 15–41, 2000.
14. Gautier, C.; Diak, G.; and Masse, S.: "A Simple Physical Model To Estimate Incident Solar Radiation at the Surface From GOES Satellite Data," *J. Appl. Meteor.*, Vol. 19, pp. 1005–1012, 1980.
15. Diak, G.R.; and Gautier, C.: "Improvements to a Simple Physical Model for Estimating Insolation From GOES Data," *J. Climate Appl. Meteor.*, Vol. 22, pp. 505–508, 1983.
16. Holt, F.C.; and Olsen, S.R.: *GOES Products and Services Catalog, NOAA/NESDIS*, 2d ed., 152 pp. U.S. Department of Commerce, Washington, DC, 1999.
17. Rao, C.R.N.; Chen, J.; Sullivan, J.T.; et al.: "Post Launch Calibration of Meteorological Satellite Sensors," *Adv. Space Res.*, Vol. 23, pp. 1357–1365, 1999.
18. Coulson, K.L.: "Characteristics of the Radiation Emerging From the Top of a Rayleigh Atmosphere, 1 and 2," *Planet. Space Sci.*, Vol. 1, pp. 256–284, 1959.
19. Allen, C.W.: *Astrophysical Quantities*, 291 pp., Athlone Press, London, England, 1963.
20. Lacis, A.A.; and Hansen, J.E.: "A Parameterization for Absorption of Solar Radiation in the Earth's Atmosphere," *J. Atmos. Sci.*, Vol. 31, pp. 118–133, 1974.
21. Paltridge, G.W.: "Direct Measurement of Water Vapor Absorption of Solar Radiation in the Free Atmosphere," *J. Atmos. Sci.*, Vol. 30, pp. 15–160, 1973.
22. "The SURFRAD Network," National Oceanic and Atmospheric Administration (online), URL: <http://www.srrb.noaa.gov/surfrad> Last Accessed February 17, 2004.
23. Jedlovec, G.J.: "Determination of Atmospheric Moisture Structure From High-Resolution MAMS Radiance Data," Ph.D. Dissertation, University of Wisconsin-Madison, Madison, WI, 1987.
24. Guillory, A.R.; Jedlovec, G.J.; and Fuelberg, H.E.: "A Technique for Deriving Column-Integrated Water Content Using VAS Split Window Data," *J. Appl. Meteor.*, Vol. 32, pp. 1226–1241, 1993.
25. Suggs, R.J.; Jedlovec, G.J.; and Guillory, A.R.: "Retrieval of Geophysical Parameters From GOES: Evaluation of a Split Window Retrieval Technique," *J. Appl. Meteor.*, Vol. 37, pp. 1205–1227, 1998.
26. Suggs, R.J.; Jedlovec, G.J.; Lapenta, W.M; et al.: "Evaluation of Skin Temperatures Retrieved From GOES-8," Preprint, *10th Conference of Satellite Meteorology and Oceanography*, Amer. Meteor. Soc., Long Beach, CA, pp. 137–140, 2000.

27. Suggs, R.J.; Lapenta, W.M.; Jedlovec, G.J.; et al.: "Intercomparison of GOES-8 Imager and Sounder Land Surface Temperature Retrievals," Preprint, *11th Symposium on Meteorological Observations and Instrumentation*, Amer. Meteor. Soc., Albuquerque, NM, pp. 362–365, 2001.
28. McNider, R.T.; Song, A.J.; Casey, D.M.; et al.: "Toward a Dynamic-Thermodynamic Assimilation of Satellite Surface Temperature in Numerical Atmospheric Models," *Mon. Weather Rev.*, Vol. 122, pp. 2784–2803, 1994.
29. Garand, L.; Turner, D.S.; Larocque, M.; et al.: "Radiance and Jacobian Intercomparison of Radiative Transfer Models Applied to HIRS and AMSU Channels," *J. Geophys. Res.*, Vol. 106, pp. 24,017–24,031, 2001.
30. Menzel, W.P.; Smith, W.L.; and Stewart, T.R.: "Improved Cloud Motion Wind Vector and Altitude Assignment Using VAS," *J. Appl. Meteor.*, Vol. 22, pp. 377–384, 1983.
31. Schreiner, A.J.; Unger, D.A.; Menzel, W.P.; et al.: "A Comparison of Ground and Satellite Observations of Cloud Cover," *Bull. Amer. Meteor.*, Vol. 74, pp. 1851–1862, 1993.
32. Suggs, R.J.; Haines, S.L.; Jedlovec, G.J.; et al.: "Land Surface Temperature Retrievals From GOES-8 Using Emissivities From MODIS," Preprint, *12th Conference on Satellite Meteorology and Oceanography* (CD-ROM), P4.19, Amer. Meteor. Soc., Long Beach, CA, 2003.

| REPORT DOCUMENTATION PAGE | | | <i>Form Approved OMB No. 0704-0188</i> | |
|---|---|---|--|--|
| Public reporting burden for this collection of information is estimated to average 1 hour per response, including the time for reviewing instructions, searching existing data sources, gathering and maintaining the data needed, and completing and reviewing the collection of information. Send comments regarding this burden estimate or any other aspect of this collection of information, including suggestions for reducing this burden, to Washington Headquarters Services, Directorate for Information Operation and Reports, 1215 Jefferson Davis Highway, Suite 1204, Arlington, VA 22202-4302, and to the Office of Management and Budget, Paperwork Reduction Project (0704-0188), Washington, DC 20503 | | | | |
| 1. AGENCY USE ONLY (Leave Blank) | 2. REPORT DATE June 2004 | 3. REPORT TYPE AND DATES COVERED Technical Memorandum | | |
| 4. TITLE AND SUBTITLE The Geostationary Operational Environmental Satellite (GOES) Product Generation System | | | 5. FUNDING NUMBERS | |
| 6. AUTHORS S.L. Haines, R.J. Suggs, and G.J. Jedlovec | | | | |
| 7. PERFORMING ORGANIZATION NAME(S) AND ADDRESS(ES) George C. Marshall Space Flight Center Marshall Space Flight Center, AL 35812 | | | 8. PERFORMING ORGANIZATION REPORT NUMBER M-1118 | |
| 9. SPONSORING/MONITORING AGENCY NAME(S) AND ADDRESS(ES) National Aeronautics and Space Administration Washington, DC 20546-0001 | | | 10. SPONSORING/MONITORING AGENCY REPORT NUMBER NASA/TM-2004-213286 | |
| 11. SUPPLEMENTARY NOTES Prepared by the Earth Science Department, Science Directorate | | | | |
| 12a. DISTRIBUTION/AVAILABILITY STATEMENT Unclassified-Unlimited Subject Category 47 Availability: NASA CASI 301-621-0390 | | | 12b. DISTRIBUTION CODE | |
| 13. ABSTRACT (Maximum 200 words) The Geostationary Operational Environmental Satellite (GOES) Product Generation System (GPGS) is introduced and described. GPGS is a set of computer programs developed and maintained at the Global Hydrology and Climate Center and is designed to generate meteorological data products using visible and infrared measurements from the GOES-East Imager and Sounder instruments. The products that are produced by GPGS are skin temperature, total precipitable water, cloud top pressure, cloud albedo, surface albedo, and surface insolation. A robust cloud mask is also generated. The retrieval methodology for each product is described to include algorithm descriptions and required inputs and outputs for the programs. Validation is supplied where applicable. | | | | |
| 14. SUBJECT TERMS skin temperature, total precipitable water, cloud top pressure, cloud albedo, surface albedo, surface insolation, satellite retrievals | | | 15. NUMBER OF PAGES 64 | |
| | | | 16. PRICE CODE | |
| 17. SECURITY CLASSIFICATION OF REPORT Unclassified | 18. SECURITY CLASSIFICATION OF THIS PAGE Unclassified | 19. SECURITY CLASSIFICATION OF ABSTRACT Unclassified | 20. LIMITATION OF ABSTRACT Unlimited | |